Position of the Frenkel Line in supercritical nitrogen at 25°C, 75°C, 100°C and 125°C

By Abdullah Al-Maiyah

Acknowledgment: I would like to express my deepest gratitude to my parents, Dr. Mohammed Al-Maiyah and Dr. Rafah Al-Bahrani for their support as I completed this work. This is as much a product of their toil as mine. I must also thank Dr. John E. Proctor for his indispensable expertise and knowledge, which he generously shared throughout. I will also thank James Spender and Bill George, both of whom made the lab work much less lonely when they were around. Finally, I will thank Rahul Vaghmaria and Tessa Noble, both of whom encouraged me during the most stressful days of the project.

Abstract: The pressure at which the Frenkel line was crossed in supercritical nitrogen was investigated at different temperatures via Raman spectroscopy, using a diamond anvil cell to control pressure and ruby or Sm:YAG as a pressure scale. The results for the lower two temperatures clearly follow the expected trend of a higher pressure crossing at higher temperature, but the last two gave inaccurately low results, probably caused by the high temperatures lowering the pressure scale's fluorescence intensity to the point of making the peak wavelength difficult to accurately determine. Nonetheless, the results do suggest higher temperatures cause higher pressure Frenkel line encounters, as expected.

Introduction:

The traditional *P,T* phase diagram separates the three states of matter encountered in everyday life, solids, liquids and gases, in order of descending density; this view of matter remains practical at subcritical *P,T* conditions. Beyond the critical point, the matter enters a supercritical fluid state, previously thought to have no qualitatively different phases [1], only responding to *P,T* condition changes with continuous expansion or contraction. This view has since been challenged by experimental evidence of "narrow" *P,T* ranges within which intermediate supercritical states occur (the term "narrow" is used in ref. [2] to differentiate from changes over a "wide distribution"; instead, "narrow" refers to a transition more similar to a "definite line", to quote ref.[2]). The traditional picture has the gas and liquid states separated by the vapour pressure curve and the liquid and solid states separated by the melting curve. The transitions between a gas and liquid or liquid and solid states of matter are abrupt, first-order phase transitions, involving latent heat. In such a case, the matter will absorb (before evaporation or melting) or release (before condensation or freezing) a discrete, particular amount of energy, fixed based on the amount of matter in transition. Despite the energy flow, the temperature of the matter sample will not change until the transition is complete; for example, melting ice will continue absorbing heat, but will remain at 0°C until it has melted into water, at which point further energy will begin to raise its temperature. [3] The above makes it easy to determine under what exact *P,T* conditions such a transition occurs, as temperature will abruptly stop changing until the transition is complete.

Conversely, the transitions between different supercritical states at higher *P,T* conditions are narrow and non-first order. By non-first order, it is meant that the transition causes no discontinuity in the matter's thermodynamic variables. One such transition, the Widom lines, is in some ways loosely like a continuation of the vapour curve. When subcritical matter crosses the vapour pressure curve, it displays a spike in compressibility caused by changes in density and viscosity. These spikes persist beyond the critical point when crossing the Widom lines, but decrease in magnitude the higher above the critical point the *P,T* conditions become, smearing out the spikes [4]. The result is that the Widom lines only exist relatively close to the critical point [5].

The transition being studied in this project, known as crossing the Frenkel line [2], is between two supercritical states: “rigid-liquidlike" and “gaslike” (defined in next paragraph). This transition involves no latent heat, with the matter simply approaching the Frenkel line until it is crossed. Also different from a subcritical liquid-gas transition is that there is no sudden, discontinuous change in density upon crossing the Frenkel line. An isothermal range of pressures and their density values are shown in **Figure.1** and, despite the Frenkel line being crossed (at room temperature, 25°C, N_2 will cross the Frenkel line at approximately 140 MPa [6]), no sudden change in density is apparent. Note, density does slightly rise, but this is mostly a simple consequence of the higher pressure and lower volume and not the huge increase that would be seen in a subcritical gas condensing into a subcritical liquid. The table itself is part of a larger table created using an online tool [7] using equations of state from the cited paper [8].

a)

Temperature (C)	Pressure (MPa)	Density (mol/l)	Volume (l/mol)	Internal Energy (kJ/mol)
25.000	120.00	21.896	0.045671	3.3247
25.000	125.00	22.216	0.045012	3.2904
25.000	130.00	22.524	0.044397	3.2580
25.000	135.00	22.819	0.043823	3.2276
25.000	140.00	23.103	0.043284	3.1989
25.000	145.00	23.376	0.042778	3.1718
25.000	150.00	23.640	0.042301	3.1461
25.000	155.00	23.895	0.041850	3.1219
25.000	160.00	24.141	0.041422	3.0990

b)

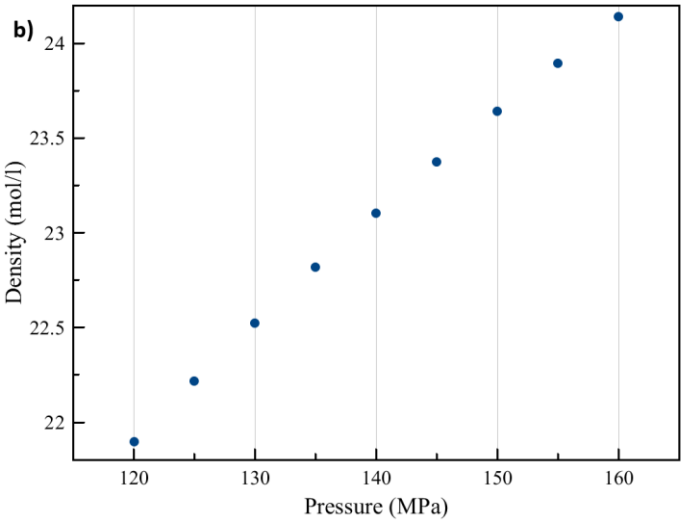

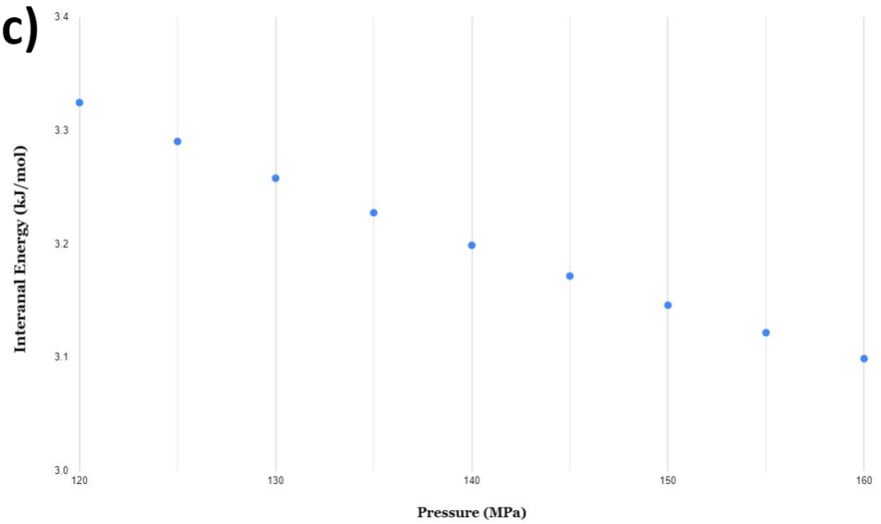

Figure.1: A screen capture of the table, a) showing the associated pressure values of 25°C N_2 crossing the Frenkel line, at approximately 140 MPa. It is apparent from the graph plotted from this data, b) that no sudden change in density occurs in crossing this boundary from gaslike supercritical fluid to rigid-liquidlike, only the same gradual increase primarily due to increased pressure that can be seen throughout the whole range. Likewise, graph c) shows no discontinuity in internal energy at the Frenkel line crossing.

In the context of supercritical fluids, “rigid-liquidlike” (sometimes referred to as just “liquidlike”) and “gaslike” are essentially descriptions of the *P,T* boundaries between the sudden emergence of liquidlike or gaslike behaviours.
These behaviours include the following: firstly, molecules in a rigid-liquidlike supercritical fluid vibrate about a number of fixed points, like in a solid, whereas a gaslike supercritical fluid’s molecules move via ballistic motion. Note, while liquids do oscillate about fixed points, these points can shift and change, unlike in solids. Additionally, while there is no sudden change in density (as described above and as demonstrated in **Figure.1**) or compressibility, there is a change in how compression is achieved; on the gaslike side, it is achieved via gaps around individual molecules being filled by others, increasing the coordination number (the number of immediate neighbours each molecule has) the more the fluid is compressed. On the rigid-liquid side however, the coordination number is unchanged throughout compression; instead, compression is achieved by forcing already neighbouring molecules closer together [9], opposing intermolecular repulsion.
Another behavioural difference is the effect of pressure on Raman detectable vibration frequencies. These frequencies are the result of Raman scattering. Incident light can be scattered by a given material, in this case nitrogen molecules, in three ways: reflection or Rayleigh scattering, which are elastic, or, relevant here, Raman scattering, which is inelastic. While the other two are far more likely to occur (reflection being overwhelmingly the most common, followed by Rayleigh scattering), Raman scattering is special as it changes the wavelength of the scattered light. By using a monochromatic, coherent light like a laser, of a known wavelength, on a sample and then filtering out scattered light of that same wavelength, only the

inelastically, Raman scattered photons are detected. The degree of this “Raman shift” gives information about the scattering material. The relevant information in this project is as follows: the behaviour on the rigid-liquid side of the Frenkel line is that the Raman detectable vibration frequencies produced by the nitrogen molecules increase as pressure does. Such behaviour is typical of liquids and solids as the interatomic forces between neighbouring molecules in such materials is repulsive. This repulsion increases as pressure does (due to the compression forcing molecules closer as described above), in turn driving up the frequency of Raman detectable vibrations. In the *P,T* region on the gaslike side of the Frenkel line however, the opposite relationship between pressure and vibrational frequency is apparent. At these lower pressures, molecules are not forced as close together and thus the repulsive forces between them are far less in magnitude. Instead, it is the attractive van der Waals forces between molecules that dominate. Note, in both states mentioned these two factors, repulsive interatomic forces and attractive van der Waals forces, are competing. The change in relationship overall is simply as a result of one factor overtaking the other as the dominant factor acting on the molecules.

Because of the multitude of effects described above, any experiment that aims to determine these transitional parameters must closely monitor the sample across controlled, minute pressure adjustments (in practice, these adjustments were around 0.1-0.005 GPa).

As the molecules in a given sample move more energetically at higher temperatures, resulting in a lower density, the transition between gaslike behaviour and rigid-liquidlike behaviour is expected to occur at a higher pressure for a higher temperature sample, all other properties being equal, as a higher pressure is required to achieve the required density to cross the Frenkel line. The crossover could be detected by looking for the change in effect of pressure on Raman detectable vibration frequencies described earlier. The following experiments set out to test this.

Experimental Methodology:

To examine the effect of temperature on supercritical nitrogen’s Frenkel line, data was gathered at three temperatures: 75°C, 100°C and 125°C. Data for a fourth temperature, 25°C, collected as part of a previous series of experiments [10] was also used, with permission from the original author. This range of temperatures was chosen was not covered in prior similar experimental result, such as those discussed in ref.[10] and could experimentally test and extend the estimated path of the Frenkel line from such experiments, as shown in **Figure.2**.

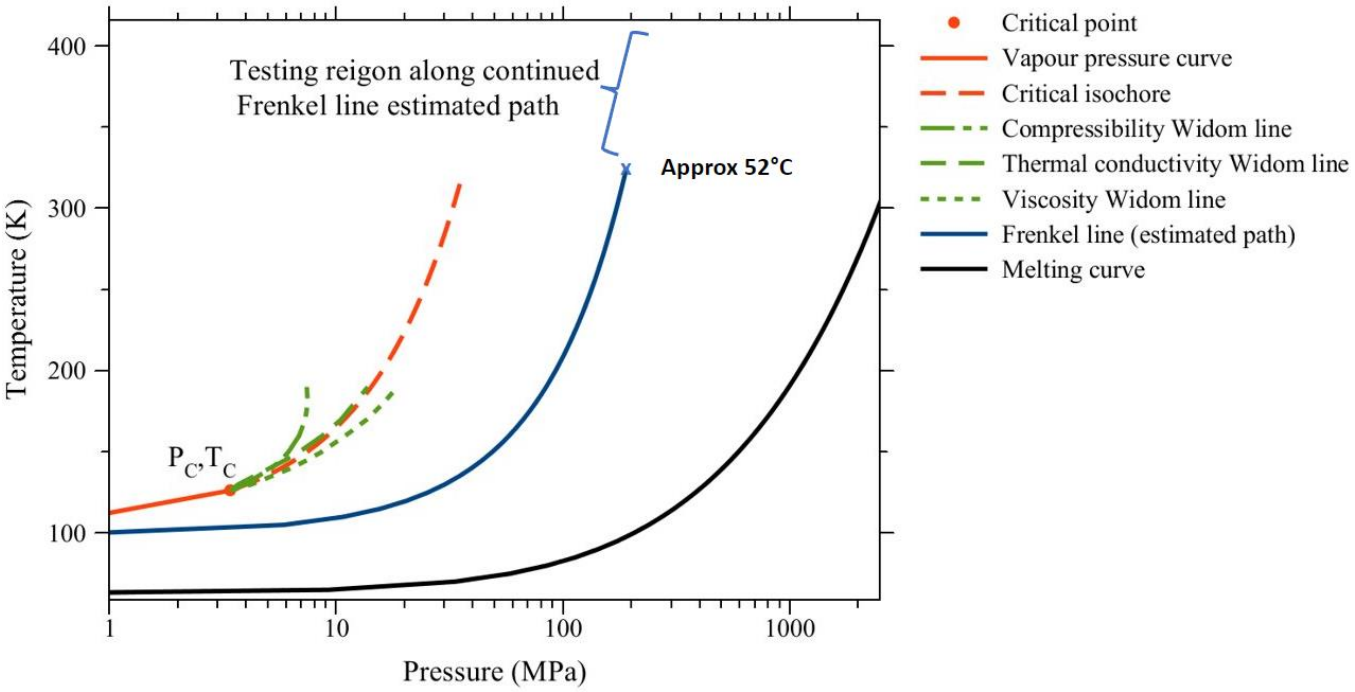

Figure.2: A phase diagram of nitrogen based on data from ref.[10] showing an estimated Frenkel line path (dark blue). The highest temperature on this line is 325K, approximately 52°C. This project aims to experimentally extend this line beyond this temperature.

While the aim of this project is to extend the nitrogen phase diagram shown above, it is worth noting that the heating equipment available during this project's experiments was not capable of reaching and maintaining temperatures above 125°C, thus limiting the temperatures that could be tested at. The temperatures of 75°C, 100°C and 125°C were deemed worth studying (being higher than 52°C) whilst also atainable with the equipment available.

The experiments were conducted using piston-cylinder diamond anvil cells (DACs) made of maraging steel. The maraging steel can be heated up to the target temperatures, and indeed far beyond, without expanding to an extent that would compromise the DAC's seal.

Firstly, the cell is prepared by cleaning the diamonds with acetone, ensuring minimal contaminants end up in the final sample. The cell is then fitted with a 200μm thick stainless steel gasket, "drilled" via EDM (electrical discharge machining) using both the method and the individual EDM machine described in ref. [11]. This gasket is created by indenting the steel with the 600μm diameter diamond culets, the centre of which is "drilled" to produce a small hole, approximately 0.2mm in diameter. Use of EDM for DAC anvil production goes back decades [12] and remains a reliable way of producing bespoke gaskets for DAC experiments.

The heating and spectroscopy took place on the custom apparatus set depicted in **Figure.4** and **Figure.5**. This apparatus has previously been used in similar experiments to good effect [13]. The DAC was placed in a mount with vernier screws able to move the DAC in all directions; these were used to finely manoeuvre the cell until aligned with the incoming lasers and the visible light view camera's fixed point

of focus. This was done while observing a real time digital feed through the camera while the sample was illuminated by a white light.
The DAC sample chamber is composed of the two opposed diamond culets compressing the area bounded by the gasket hole. A fluorescence pressure reference standard is placed in the chamber to allow for measurements of internal pressure. Similar to other heated DAC experiments, the pressure scale should be selected with considerations of the experimental temperature; while ruby would serve as a pressure scale [14] at the relatively cool 75°C, it is known to grow inaccurate at higher temperatures, thus samarium doped yttrium aluminium garnet (Sm:YAG) crystal shards were used instead [15] for the 100°C and 125°C experiments. The DAC is shown in **Figure.3**.

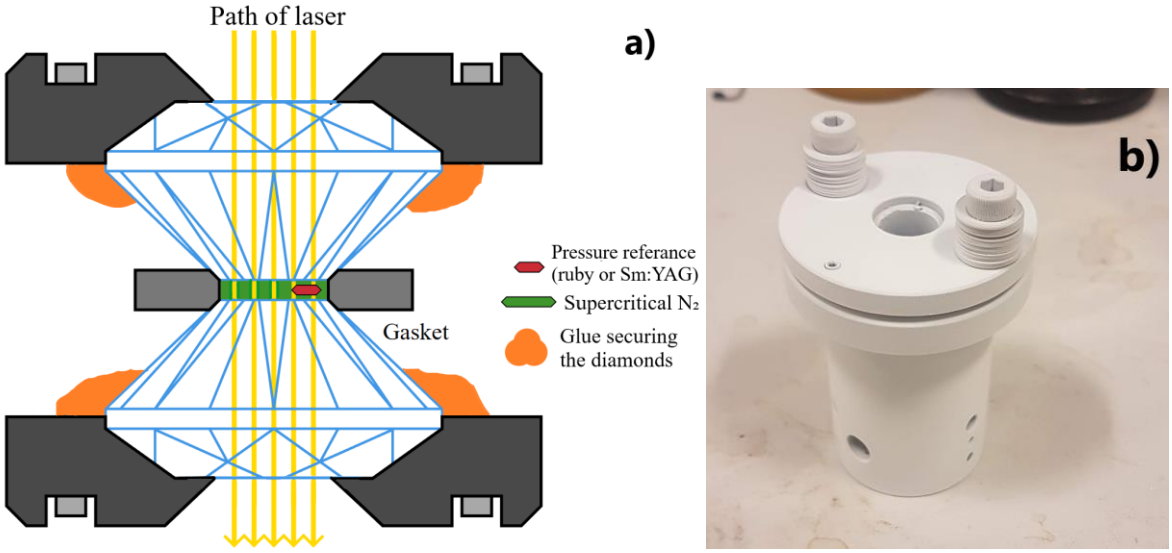

Figure.3: A cross-section diagram of the DAC's pressure chamber, a) showing how the sample is contained using the steel gasket (grey) and two diamond culets. The glue (orange) goes all the way around the diamond bases. The photograph, b) shows the individual DAC used for all readings, aside from the 25°C ones. It is white with frost after immersion in and filling with liquid nitrogen.

Once an appropriate pressure scale was selected, it had to be placed in the chamber; this was done by hand using a fine needle to pick up and manipulate a small shard of pressure scale crystal. The shards were microscopic, approximately 0.02-0.05mm across at their widest, and had to be manipulated under an optical x20 microscope while silhouetted with a backlight. They were placed off centre in the cells so that while they may be easily found during an experiment when a pressure reading needed to be taken, they could also be easily avoided when taking a nitrogen Raman spectrum; if a nitrogen reading was attempted with laser light also falling on a pressure scale shard, the resulting induced fluorescence would completely wash out any nitrogen spectrum; this is avoided by simply pointing the laser at space visibly containing only nitrogen.

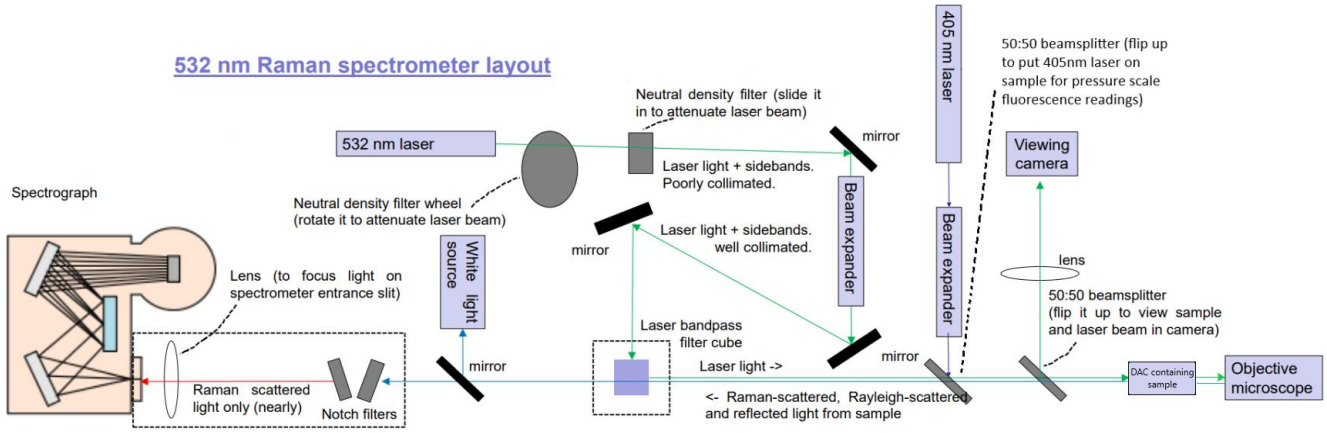

Figure.4: The schematic layout of the Raman spectroscopy apparatus, lasers and mirror arrays. The white light source was used for illumination during focusing and aligning and was deactivated before taking readings. Filters for the 532nm laser are likewise engaged while aligning and focusing, then removed before taking readings. The DAC sat in a custom brace behind the objective microscope and was manoeuvred into its optical focal point.

With the shard in position, the cell is then immersed in a bath of liquid N_2 while open, then closed while still immersed. The pressure screws can then be tightened to keep the N_2 stable in liquid state, even at ambient or higher temperatures, via pressure. At this point it can be easily transported, so long as the pressure screws are not undone. Note that the temperature difference between the room temperature DAC and the supercooled liquid nitrogen will cause the nitrogen to rapidly boil around the immersed DAC until the cell's own temperature equilibrates with that of the nitrogen. Liquid nitrogen will be lost due to evaporation during this and should be topped up as needed. An advantage of this system is the prevention of contamination from air; both carbon dioxide and oxygen are Raman active and thus may otherwise appear in any spectra.

The cell would now be mounted onto the spectroscopy apparatus in a compressing lever-arm. After the lever is set up, the cell is fitted with a resistive pipe-heater sleeve. The heater sleeve is fitted around the protruding cell cylinder and tightened with screws to ensure good thermal contact for efficient and even heat transfer. The contact thoroughness can be tested with a small piece of paper, using it to probe for gaps under the heater.

At this point, before beginning to heat, the pressure should be transferred to the lever arm, so as not to risk deformation of the pressure screws. The arm was gradually tightened until a pressure scale fluorescence check revealed a notable increase and the pressure screws were then removed.

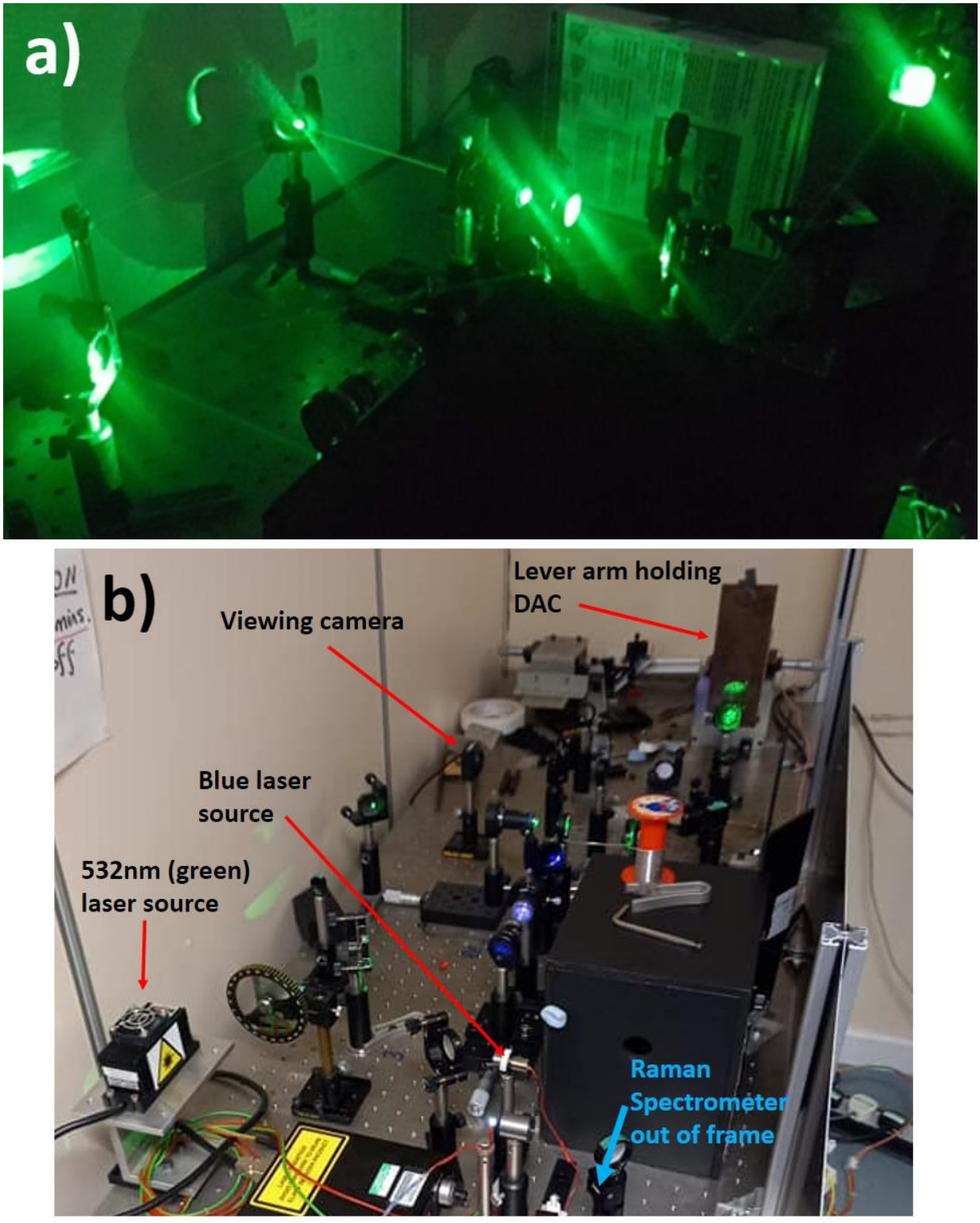

Figure.5: Image a) shows the 532nm laser in use. The DAC in its mount is visible in the top-right and the large dark shape in the lower centre is the bandpass filter cube's casing. The lens array in the centre of the image is the beam expander. Image b) is a labelled photograph showing the same equipment.

As this project studies the effect of different temperatures on the Frenkel line, a steady temperature over the course of an experiment is a hard requirement; to this

end, measurements can only be carried out once temperature have stabilised at the target level. As the cell's sample chamber is far too small to contain a thermocouple (and the fact no thermocouple could withstand the pressures within), the temperature of the cylinder diamond was taken instead with the assumption that if the DAC was held at this temperature steadily for short while (in practice approximately 15 minutes) the sample would also equilibrate at this temperature. The assumption is based on the high thermal conductivity of diamond. External temperature was monitored by using a handheld thermocouple probe and multimeter, held onto the exposed back of the cylinder diamond. Current supplied to the heater must be finely adjusted so that this equilibrium occurs at the target temperature. This was done by manipulating a custom-built controller for the heater, also successfully used in previous experiments [13]. Temperature should be checked constantly during this process via thermocouple probe, and the current adjusted accordingly, until temperature reads constant at the target for at least 10 seconds.

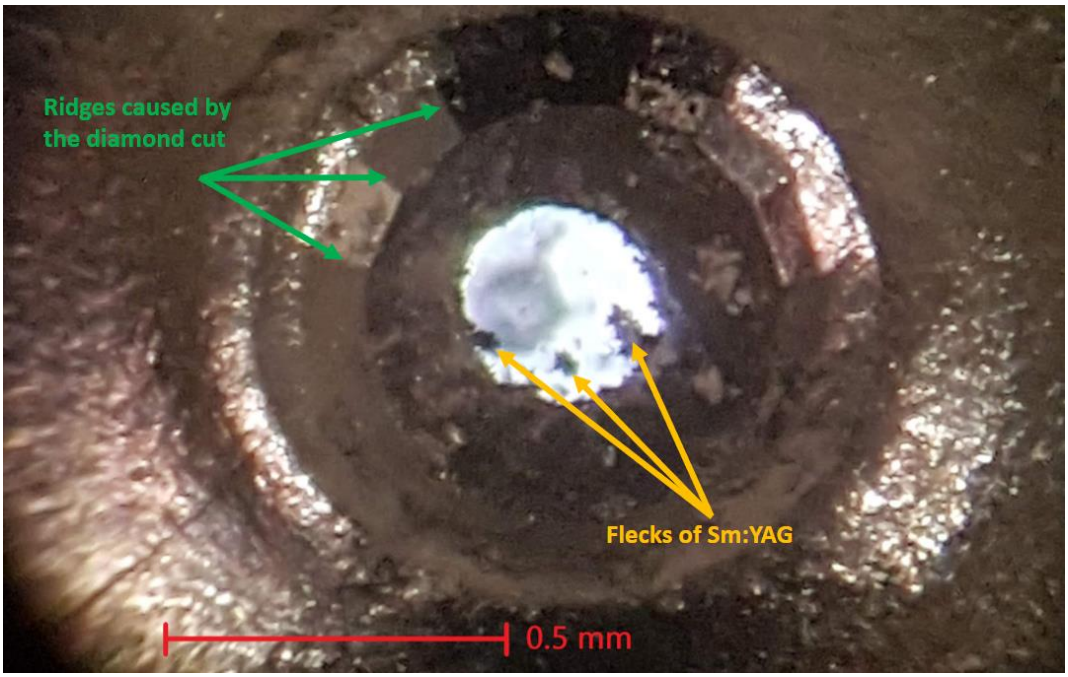

Figure.6: A photograph of a prepared gasket, taken through a 20x magnification microscope. The flat indented surface is 0.6mm in diameter, matching the diamond culet that formed it. Note the ridges in the indentation walls, caused by the cut of the diamond. The small dark flecks in the bottom-left, bottom-middle and larger fleck at bottom-right of the hole are small shards of pressure scale crystal, in this case Sm:YAG, positioned away from the centre to be easily avoided when taking nitrogen Raman spectra. The larger, slightly lighter mark in the middle-left of the hole is simply dirt on the back of the diamond and is out of focus when readings are taken. The impact of such contaminants is mostly negligible.

Once the lever arm is supplying the pressure and the DAC has reached the target temperature, the experiment can begin. The lever arm's pressure is slightly relieved by fractionally undoing the screw, the DAC is refocused in the apparatus and a pressure scale fluorescence spectrum is taken while being excited by the 405nm laser. Then, a Raman spectrum of the supercritical nitrogen is taken using the

532nm laser. Finally, a second pressure scale reading is taken with the 405nm laser. These spectra are collected as intensity, in individual detector counts, over wavelength in nanometers. At this point, the pressure can be further relieved and the above measurements repeated until the nitrogen Raman peak disappears, indicating the cell has opened and the nitrogen has vented (**Appendix 1.7**). A final pressure scale spectrum is taken (to use as an atmospheric reference at the target temperature) and the experiment ends.

Analytical Process and Results:

The theoretical basis for the analysis of the collected data is as follows: as described in the introduction above, supercritical fluids can behave differently, according to the side of the Frenkel line they are on. The Raman detectable vibration frequencies increase with pressure on the rigid-liquid side. On the gaslike side, increased pressure lowers resulting frequencies.
When the wavenumber derived from the Raman vibrational frequency is plotted over the pressure at which they occur, a minimum appears in the data. The minimum's x-axis position can be solved for, giving the pressure value at which the sample transitions from rigid-liquidlike to gaslike, crossing the Frenkel line.
Analysis begins with pulling the raw intensity over wavelength measurements from the spectrometry software (examples shown in **Appendix 1**). These are copied to a graphing program, in this case MagicPlot, and plotted.
For pressure scale fluorescence readings, the data is fitted with Lorentzian curves over the peaks in the spectrum; for the 75°C experiment's fluorescence spectra, this is one curve for each of the characteristic two ruby peaks, as shown in **Figure.7** (further examples in **Appendix 2**). The wavelength at the centre of the higher wavelength peak is recorded and sed to calculate pressure using a calculator on the site linked in ref.[16]. These computations are based on previous academic works on fluorescence pressure scales, which are referenced on the site.
For the Sm:YAG spectra of higher temperature experiments, the peaks *Y1-4* were likewise fitted with Lorentzian distributions (examples in **Appendix 3**). For each spectrum, the wavelength value at *Y1*'s centre was recorded and, along with the wavelength of *Y1*'s centre at ambient pressure, was used to calculate pressure; this also was done using the site linked in ref.[16].
A Lorentzian fit was used as ruby [17] and Sm:YAG [18] fluorescent spectra have both been known to widen into this profile.
For both ruby and Sm:YAG, the pressure value calculator requires both the measured wavelength of the chosen fluorescence peak and a reference wavelength of the same peak at ambient pressure. This is why a final pressure scale spectrum is taken after the nitrogen is vented at the end of an experiment.
With a pressure value for before and after each nitrogen Raman spectrum, the mean of the two was used as the pressure during the nitrogen measurement.

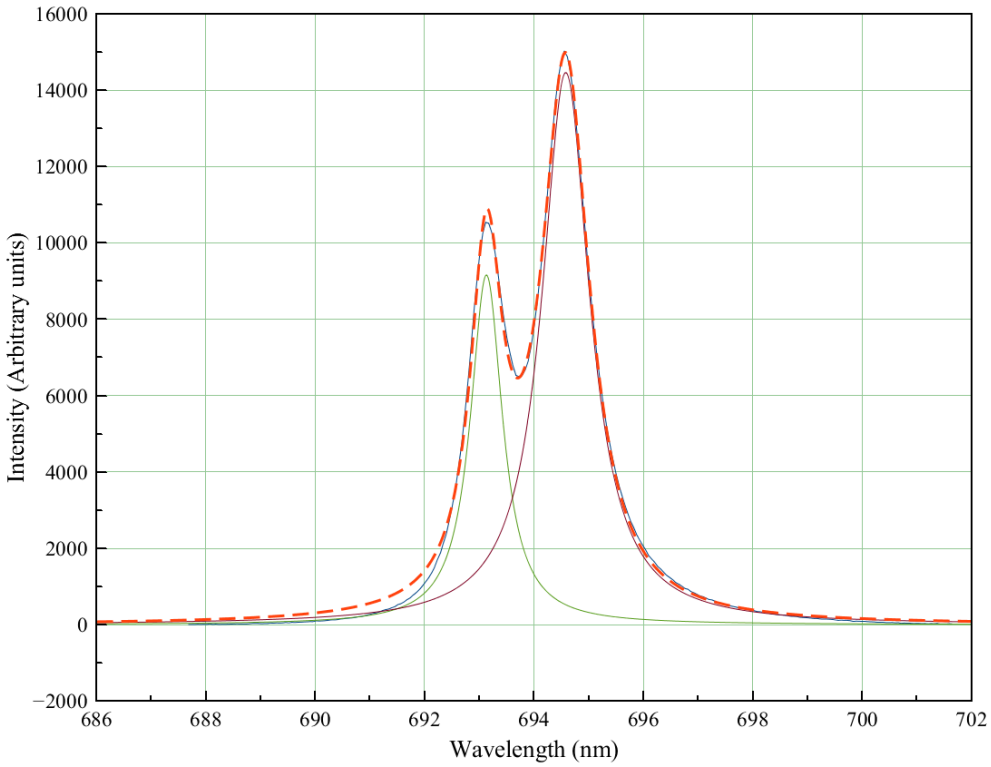

Figure.7: Example of the characteristic double peaks of ruby spectra. The peak profiles can be fit accurately enough for the purposes of a pressure reading with two Lorentzian distributions. This spectrum was recorded at ambient pressure, at 75°C.

The analysis of nitrogen Raman spectra are as follows: the wavelengths of the Raman spectra's nitrogen peaks, and their associated intensities, were recorded. These wavelengths, λ in nanometres, *nm* were converted to wavenumber, cm^{-1} with the formula below,

$$\frac{\frac{1}{532\times10^{-9}}-\frac{1}{\lambda\times10^{-9}}}{100} = wavenumber\ in\ cm^{-1} \quad (1)$$

and were plotted against intensity, as shown in **Figure.8**.

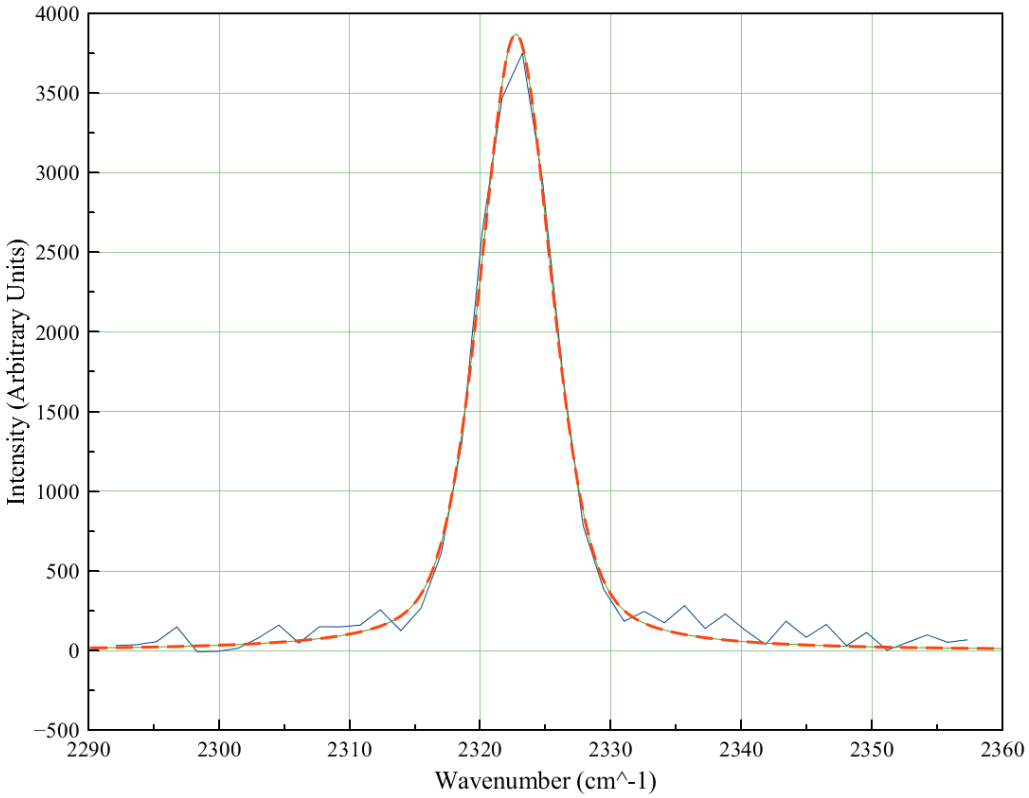

Figure.8: An example of the combined Gaussian and Lorentzian distribution around a wavenumber peak. Note that, despite the presence of both components, in proportions and magnitudes unique to each peak, the auto-fit method yielded an overall acceptable fit. This spectrum was taken at 0.809 GPa, at 76°C.

As the resulting graph's peak contains both Gaussian and Lorentzian components of comparably intensity, it cannot be accurately fit with one of these functions alone. Instead, the peaks are fitted with a pseudo-Voigt approximation fit, written in the MagicPlot graphing software as follows, where $L(A)$ is the area of the Lorentzian component of the peak, $G(A)$ is the area of the Gaussian component, x_0 is the centre of the peak's x position in cm^{-1} and dx is the width of the peak in cm^{-1}:

$$\frac{L(A)}{\pi \times dx \times \frac{1+(x-x_0)^2}{dx^2}} + \left(\frac{\ln(2)}{\pi}\right)^{\frac{1}{2}} \times G(A) \times e^{-\ln(2) \times \left(\frac{(x-x_0)^2}{dx^2}\right)} \quad (2)$$

This equation combines both Gaussian and Lorentzian functions, designed to approximate a true Voigt function.
The reason for this lies in the nature of the multitude of broadening mechanisms acting on the spectroscope's input photons; Raman scatter resulting from N_2 does not appear as purely one wavelength, despite the spectroscope's input photons being scattered by the same symmetric stretching vibration of N_2. Instead, multiple mechanisms act on the photons, to differing magnitudes, causing the distribution of intensity over wavelength to tend towards either a Gaussian distribution or a Lorentzian distribution, depending on the type of broadening mechanism. Homogeneous broadening mechanisms will broaden the peak into a Lorentzian

distribution, while inhomogeneous broadening causes a peak to follow a Gaussian distribution; there is a multitude of different examples of both homogenous, for example collision broadening [19][20], and inhomogeneous broadening, for example Doppler broadening [21] , affecting Raman spectroscopy results. Further, the 532nm laser beam itself is subject to broadening [22], contributing to the wider final peaks. The solution in this situation is that a graphing program's auto-fit feature will automatically scale the Gaussian and Lorentzian components of a pseudo-Voigt function to best fit the individual peak. Once fit, the wavenumbers at the centre of the peaks were recorded and plotted against the pressure in *GPa*, repeated for each temperature, giving the final graph for that temperature.

Upon plotting the wavenumber peaks against their pressure values, a pattern emerges: cm^{-1} values at high pressures follow a positive correlation with pressure while the opposite is true at the lowest pressures. The turning point between these two patterns shows at which point N_2 behaviour changes from rigid-liquid-like to gas-like, when the van der Waals attractive forces between molecules become the dominant effect. To determine precisely at what pressure this occurs, the equation describing the graph was first determined. As the fit had two components, a straight line (using constants a and b) and an exponential (using constants A and B), these were simply added to give the final graph fitting equation. As an example, the fitted wavenumber over pressure graph for 100°C is shown in **Figure.9**.

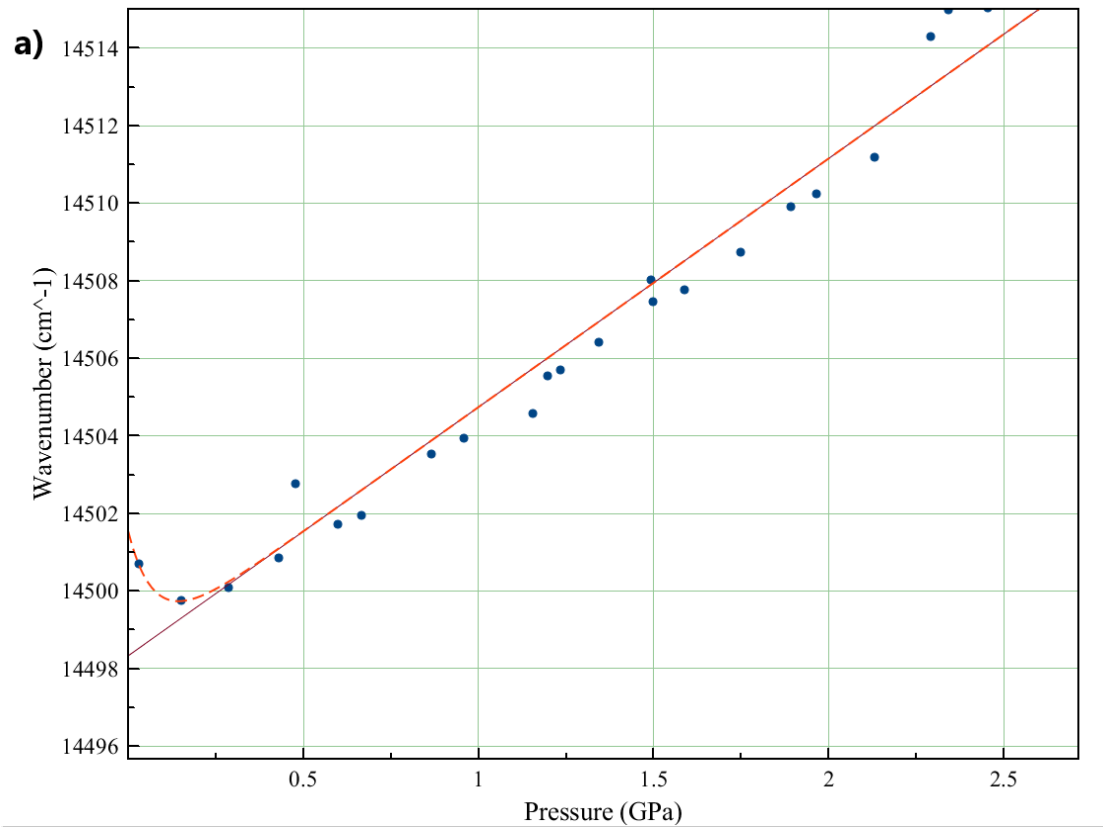
a)
Wavenumber (cm^-1)
14514
14512
14510
14508
14506
14504
14502
14500
14498
14496
0.5
1
1.5
2
2.5
Pressure (GPa)

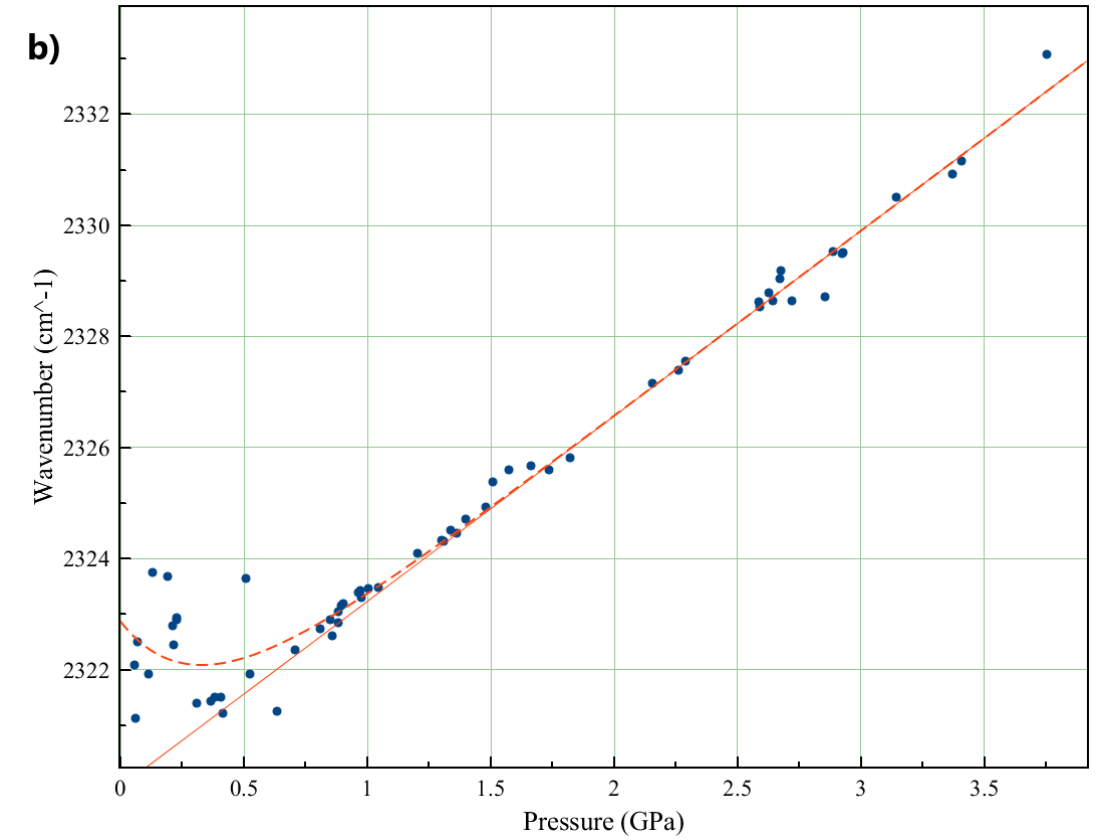
b)
Wavenumber (cm^-1)
2332
2330
2328
2326
2324
2322
0
0.5
1
1.5
2
2.5
3
3.5
Pressure (GPa)

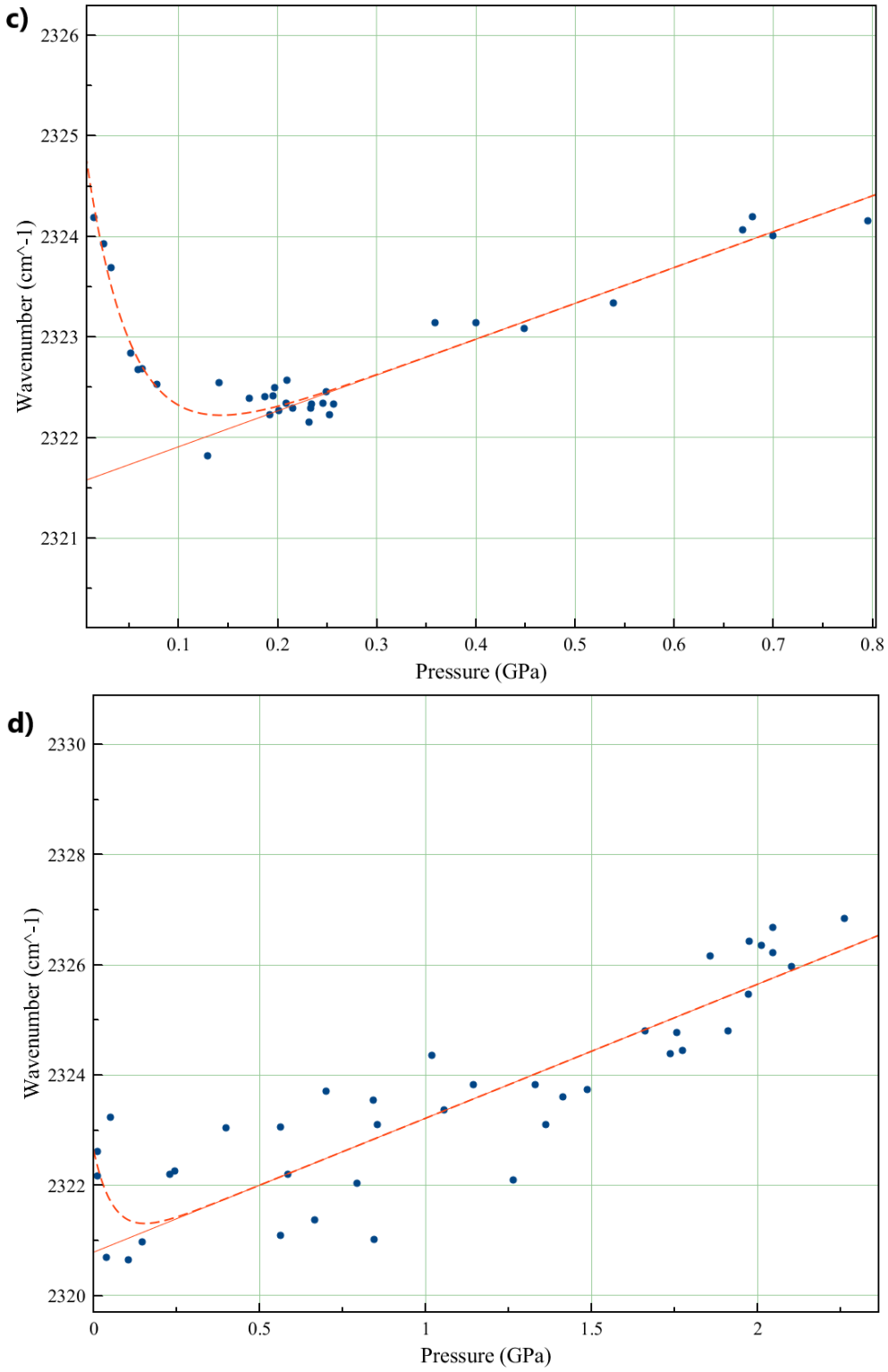

Figure.9: The graph of nitrogen Raman peak wavenumbers, for all temperatures, over their corresponding pressures in *GPa*, with those for 25°C shown in a), 75°C in b), 100°C in c) and 125°C in d). As can be seen above, the linear + exponential curve fits the data distribution well after using MagicPlot's autofit feature on it, particularly for a), b) and c). In all graphs, the point the shift in dominance between the van der Waals forces and interatomic repulsion occurs, indicating the Frenkel line crossing, is clear from the sudden near-reversal of gradient at the lower ends of the plots.

Note, as pressure is plotted on the x-axis, x here represents pressure in *GPa*. The line function is $f(x)$:

$$f(x) = ax + b + Ae^{-Bx} \tag{3}$$

Second, the equation describing the gradient of this plot was determined by differentiating the equation above:

$$\frac{d}{dx}(ax + b + Ae^{-Bx}) = a + e^{-Bx}(\frac{d}{dx}(A)) + Ae^{-Bx}(-x\frac{d}{dx}B - B) \tag{4}$$

Since both A and B are constants, their differentials are 0, thus the final gradient equation can be simplified:

$$\begin{aligned} a + Ae^{-Bx}\left(-x\frac{d}{dx}B - B\right) &= a + Ae^{-Bx}(0 - B) \\ &= a + Ae^{-Bx}(-B) = a - ABe^{-Bx} \end{aligned} \tag{5}$$

At this point, knowing that the gradient at the turning point is 0, the above equation could be rearranged and simply solved for x:

$$0 = a - ABe^{-Bx} \;\rightarrow\; x = -\frac{\ln\left(\frac{a}{AB}\right)}{B} \tag{6}$$

Finally, the values for a, b, A and B could be imputed to calculate the x, pressure value at which the turning point occurred. Again, the x-axis is in *GPa*, and so that is the unit of the results.

The calculated Frenkel line crossing pressures, to 3 decimal places, are as follows:

Temperature (°C)	Crossing Pressure (GPa)	Temp ± (°C)	Pressure ± (GPa)
25	0.143	0.05	0.1546
75	0.327	0.05	0.0205
100	0.142	0.05	0.0153
125	0.153	0.05	4.9509

The values above are compared in **Figure.10**. Note, the uncertainty in the crossing pressures is as a result of the pressure's being is calculated via auto-fit. The magnitude of uncertainty is calculated using the standard deviation values of this fit, provided by the graphing software. The uncertainty in the temperature values is ±0.05°C due to the resolution of the multimeter reading being 0.1°C.

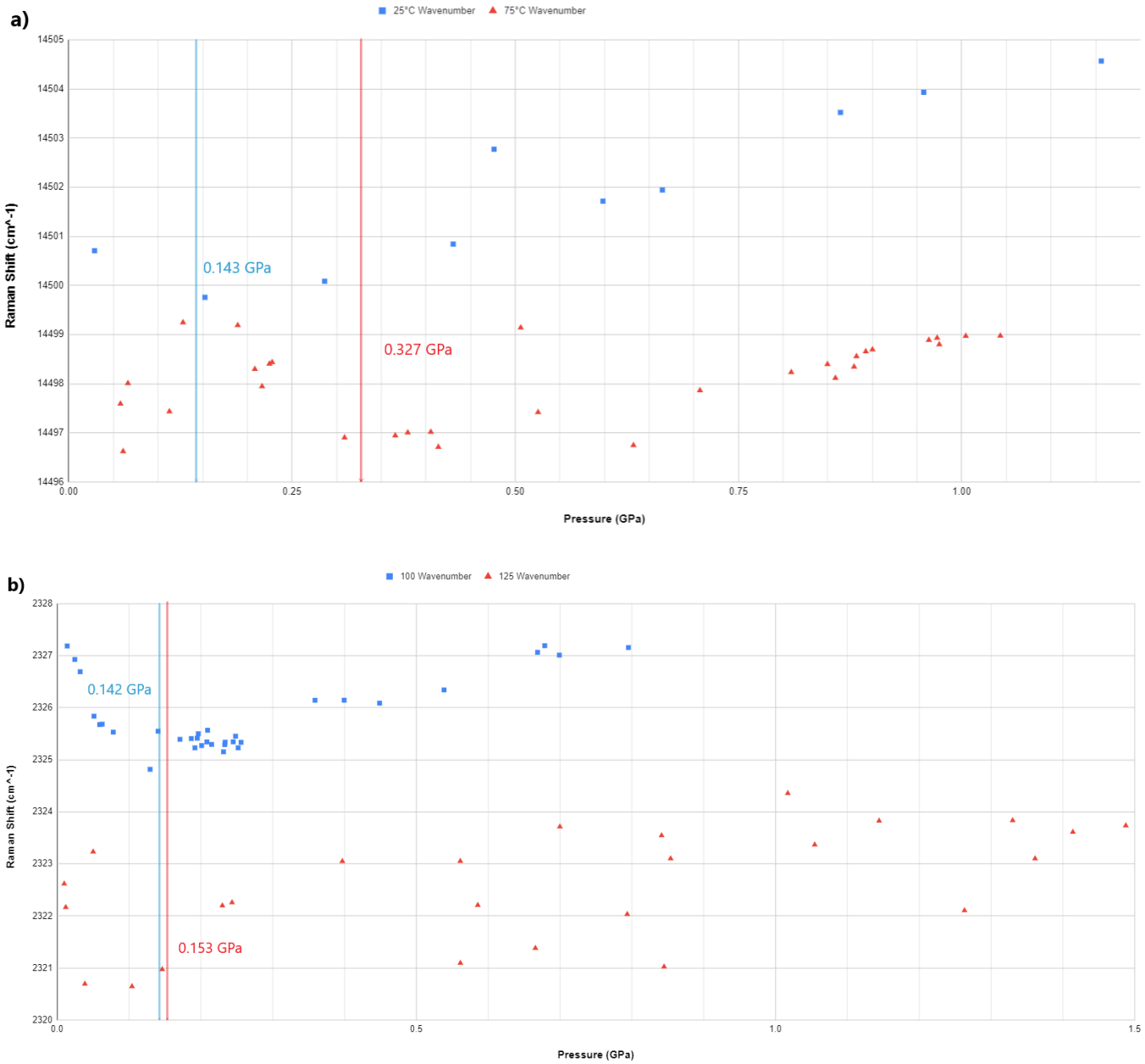

Figure.10: The temperature-induced shift in the pressure at which the Frenkel line is crossed can be seen here. Graph a) shows the datasets using ruby as the pressure scale at 25°C and 75°C. Graph b) shows the datasets using Sm:YAG as the pressure scale. While the rise between 25°C and 75°C is as predicted, the drop in pressure at the crossing between 75°C and 100°C is not the expected result, indicating some shortcoming in the experiments, particularly the means of calculating DAC sample chamber pressure. Note, while the x-axis remains to correct scale in both graphs, the 75°C data in a) and the 100°C data in b) have had their y-axis positions offset for clearer presentation.

The first thing to become apparent from these values is that, while the first two calculated values do support the expected trend, increasing crossing pressure with temperature (as explained in the fourth paragraph of the introduction), the last two values do not, the 100°C even dropping below the 25°C value. This could be seen as evidence of the expectation being incorrect and in need of revising, however,

another explanation is more likely; the fluorescence from pressure scale crystals, including the Sm:YAG used in the 100°C and 125°C experiments, is known to dim in intensity as temperature rises [23]. This is exactly the reason the Sm:YAG was used in the higher temperature experiments, as the effect is likewise known to affect ruby more harshly [23]. As shown in **Figure.11** (taken and edited from ref.[23]), YAG has a spectrum of multiple peaks positioned close to each other (*Y1*, *Y2*…). Were the peaks of low enough intensities, it is possible they would overlap and merge beyond a graphing program auto-fit's ability to accurately differentiate them. Despite this however, the fact that there is a subtle rise in calculated crossing pressure for 125°C, relative to 100°C, suggests that there was still a upward shift of the average value of *Y1* and/or *Y2*, supporting the expected trend, albeit more ambiguously than if the peaks had not merged and instead remained distinct. There was an attempt to correct for the temperature-induced intensity drop by simply increasing the spectrometer's exposure time. While this would succeed in raising the intensity counts above the background noise, it does nothing to counter the x-axis shift caused by the peaks smearing into each other, the cause of the unexpectedly low calculated pressure values for the 100°C and 125°C Frenkel line encounters.

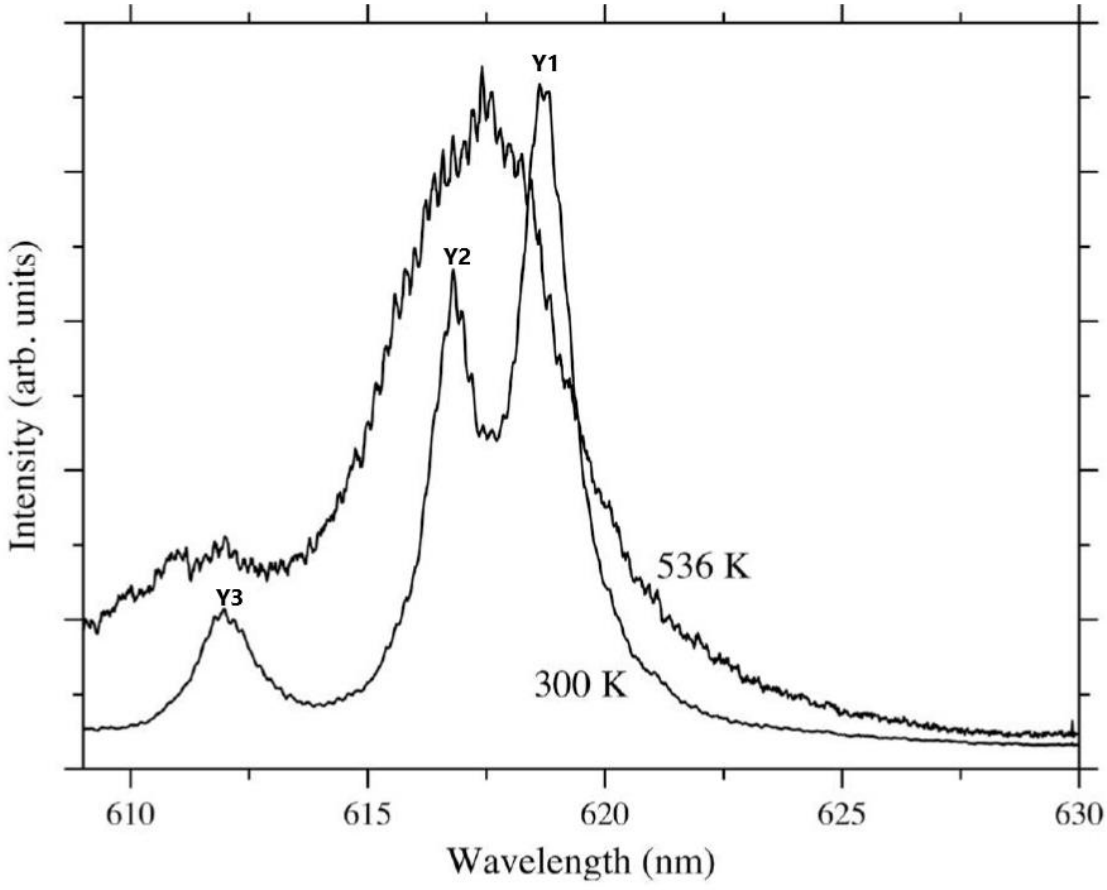

Figure.11: Two Sm:YAG fluorescence spectra, the first taken at 300K (27°C) and the second at 536K (263°C), both at 0.1 *MPa*. The increase in visible noise relative to peak intensity is a result of the much reduced peak intensity. The author points out that the 536K peaks are actually of "significantly lower" intensity and are sized up for display. Importantly for use as a pressure scale, the 536K peaks appear at a notably lower wavelength and would thus produce a lower pressure calculation, despite both peaks occurring at 0.1 *MPa*. Simply increasing exposure time, as was done in the 100°C and 125°C experiments, would do nothing to fix this shift.

Conclusion:

In conclusion, the results of this project are, unfortunately, somewhat inconclusive; on one hand, the experimental setup and method, and the analytical method are all valid means of investigating the aims of the project. The values returned for the lowest two temperatures (25°C and 75°C) are both in line with expectations of the Frenkel line crossing occurring at higher pressures when temperature is increased. However, it is clear that certain limiting factors disproportionately affected the accuracy of readings at higher temperatures (100°C and 125°C). This is most likely a result of the merging and overall dimming of fluorescence peaks of the Sm:YAG used as a pressure scale for these readings, caused by the higher temperature of the YAG pieces. While this should not qualitatively invalidate the use of YAG as a pressure scale in such experiments, the laser used to induce the fluorescence was notably low in intensity and, further, was far from ideally focused, thus the the temperature increase drove down fluorescence intensity sufficiently to make the resulting *Y1* and *Y2* peaks impossible to accurately differentiate and read, resulting in incorrectly low readings of pressure values.
To avoid the above, any future experiments using the methods of this project should use a laser of higher intensity and/or with better focusing for the fluorescent pressure reading. Such measures could keep the Sm:YAG peaks intense and distinct even at higher temperature experiments, allowing an accurate *Y1* wavelength and, as a result, an accurate pressure reading to be obtained despite the high temperature. Alternatively, a future project could take the effect into account by planning and carrying out experiments at an overall lower range of temperatures, where Sm:YAG fluorescence peak intensity would not weaken to the point of illegibility. While the difficulties with the pressure references encountered in this project suggest that DAC experiments of this kind, at temperatures around and above 125°C, may not be plausible, there exists a temperature region between approximately 50°C and 125°C that bares more thorough and accurate experimental investigation. Additionally, the effects of an improved fluorescence inducing laser may compensate for the reduced fluorescence intensity sufficiently to allow similar experiments at temperatures around and above 125°C to succeed in producing accurate pressure readings. Another point for improvement would be the method for temperature monitoring. While the use of a handheld probe was sufficiently accurate when used as part of the method described above, the potential chance for moving the DAC or shifting or

dislodging the diamond within it could cause anything from minor setbacks to complete destruction of experimental conditions, requiring a full reset or repair of the DAC itself. To eliminate this potential a thermocouple should be fitted inside the cell, as in previous experiments [13], so that a temperature value approximating that of the sample can be easily monitored. The closer this can be placed to the sample without occluding the path of lasers/visible light, the better, as this would provide a closer read to the actual sample temperature. Ideally, the read value could be close enough (within a degree Kelvin or so) to simply use as sample temperature. A fully hands-free method of reading the sample temperature at a glance would speed up both the initial heating and would make checking the temperature throughout the experiment trivial. Both factors would speed up the experiment process, potentially increasing the number of readings taken per experiment.
All the above considered, and despite the multitude of limitations, the methods used in this project have yielded evidence of the expected trend; **Figure.12** (which is based on data and figures from ref.[24]) shows that the four experimentally determined Frenkel line encounters do seem to extrapolate the Frenkel line of supercritical nitrogen.

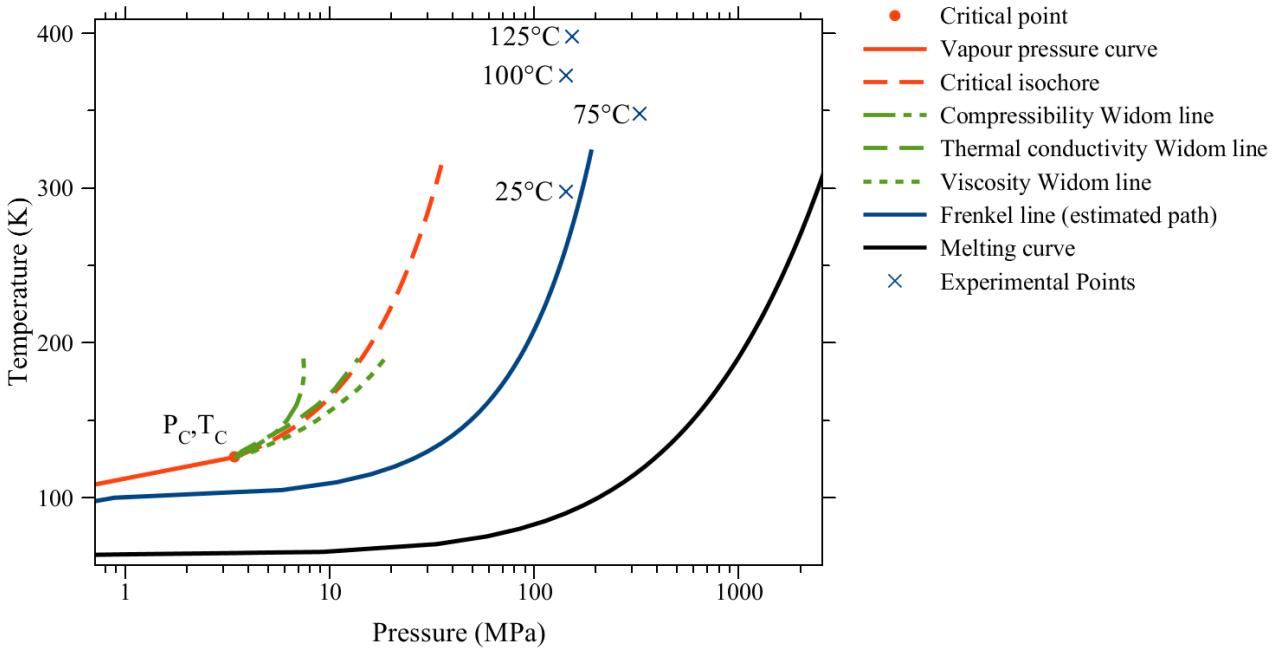

Figure.12: The four experimentally determined Frenkel line encounters displayed relative to the same prior experimentally plotted Frenkel line from **Figure.2**. Note, as explained earlier in this paper, the Frenkel line encounters at temperatures 100°C and 125°C are calculated at erroneously low pressures. These points being shifted up slightly in pressure would cause them to follow an extrapolation of the current Frenkel line even more closely.

It is the firm view of the author that a set of experiments following a similar method to that used here, taking the measures described above, would show clear evidence supporting the expected trend of a higher pressure Frenkel line encounter at higher temperature.

Appendix:

Appendix 1: Below are two examples of raw Raman spectra from each temperature experiment. As there were many such spectra involved in this project (over 100), with relatively few real differences, these spectra were chosen to be representative. Spectra for 25°C were excluded as they were provided and not directly captured.

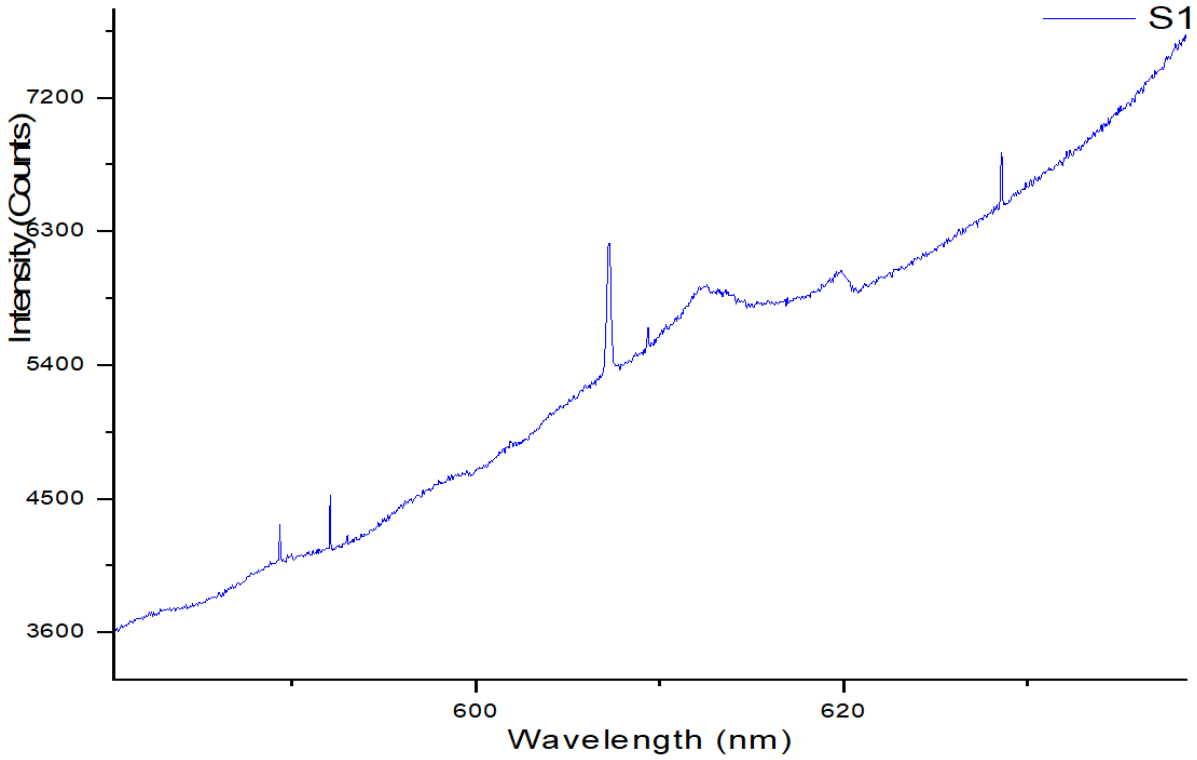

1.1: A Raman nitrogen spectrum, collected at 71°C and approximately 2.626 GPa. Inaccuracies in temperature such as this (4°C below target) are corrected for when calculating pressure. The central peak is the Raman peak while the other, smaller peaks at the edges are the result of interference such as CMBR photons.

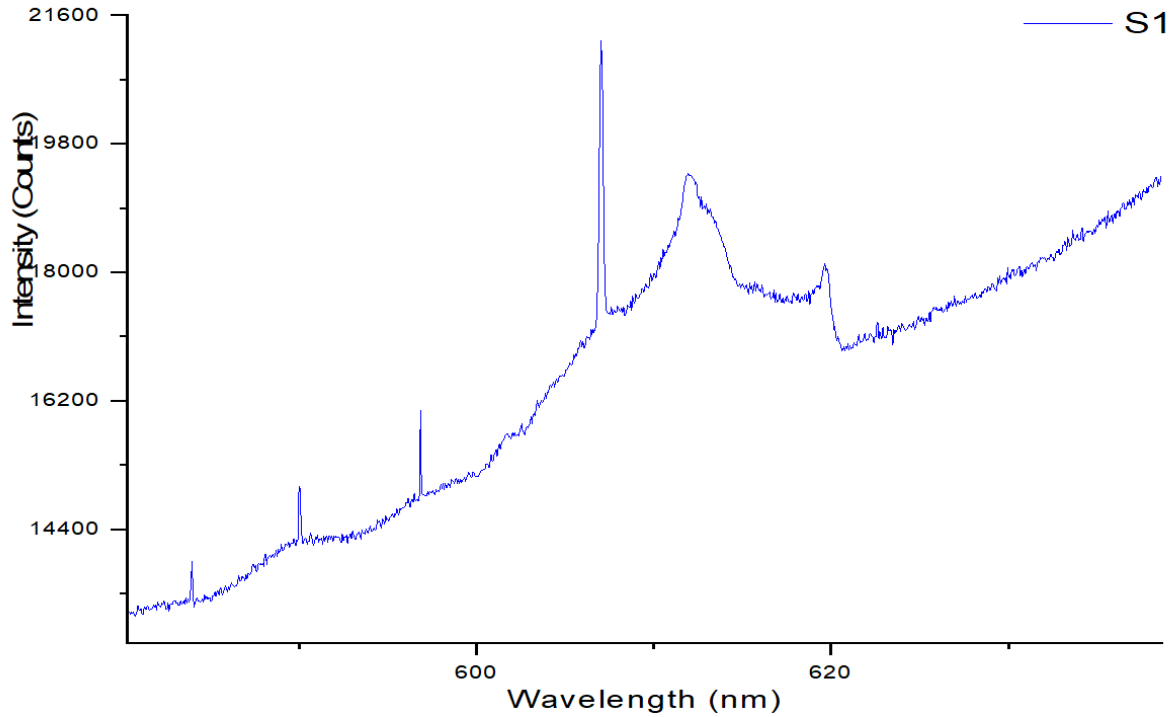

1.2: A nitrogen spectrum, collected at 75°C and approximately 0.975 GPa. Again, smaller peaks are results of interference. Only large central peak is the result nitrogen Raman scattering. This remains the case for all following spectra in **Appendix 1**.

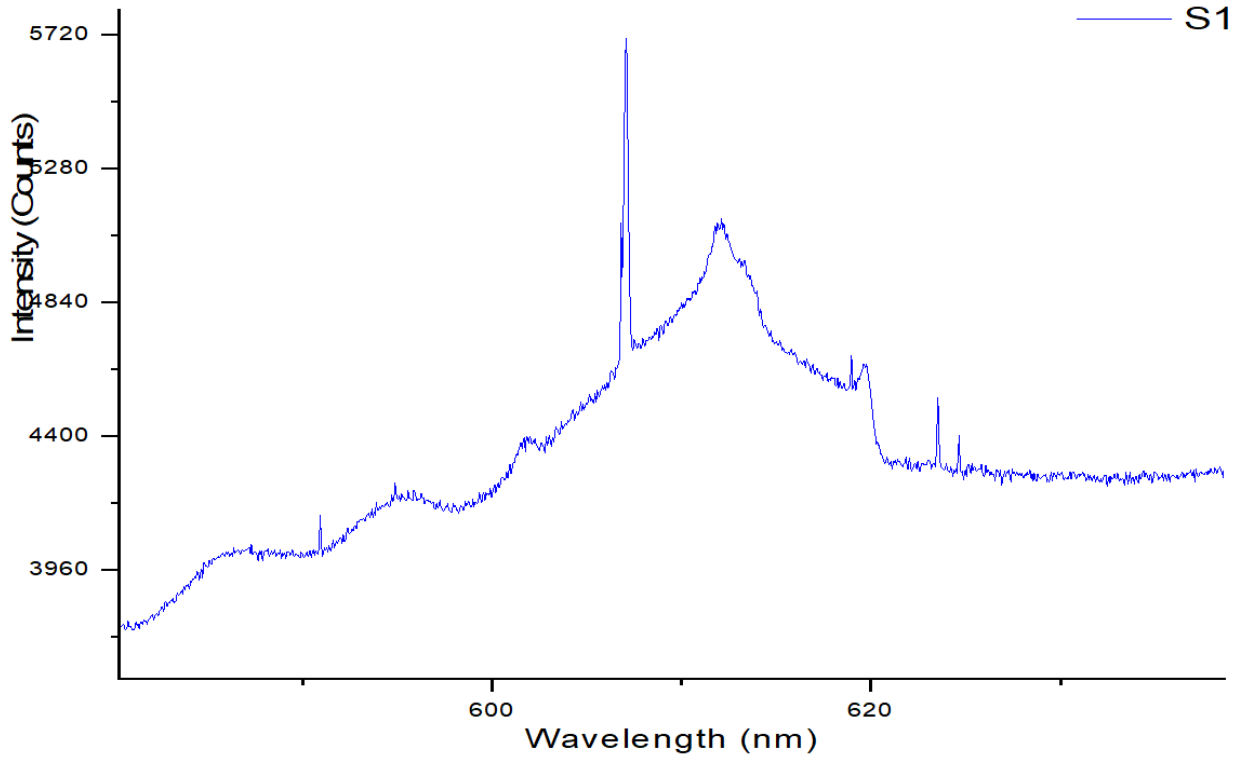

1.3: A nitrogen spectrum collected at 100°C and approximately 0.699 GPa.

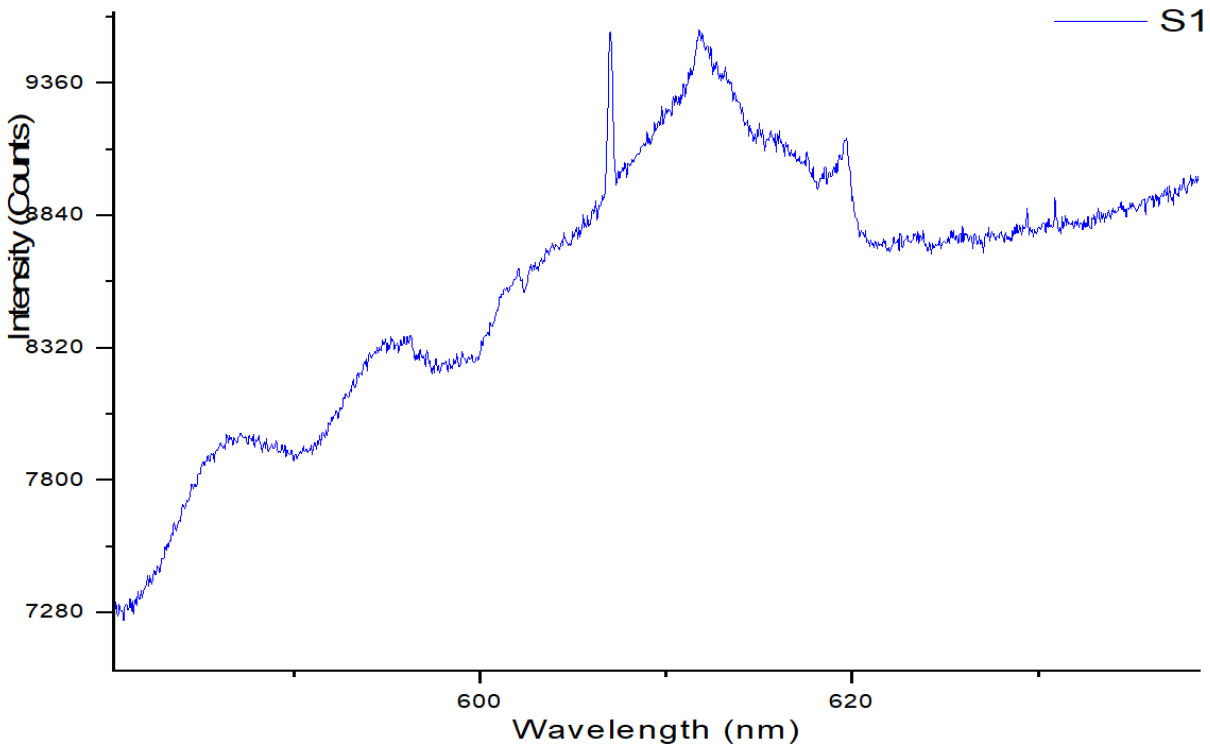

1.4: A second spectrum collected at 100°C and approximately 0.171 GPa. Note the less intense nitrogen peak (relative to background), the result of the reduced pressure. As the nitrogen molecules are less compressed, less laser light is scattered as it falls on fewer total nitrogen molecules.

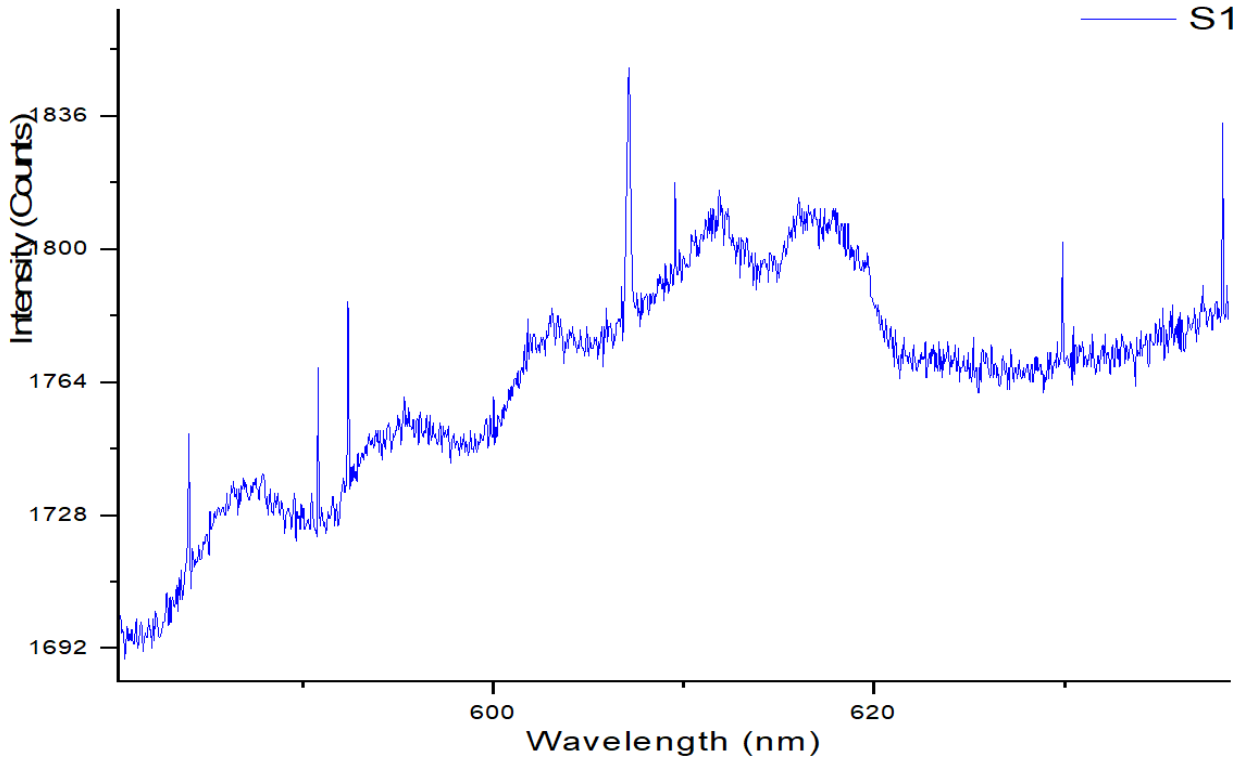

1.5: A nitrogen spectrum collected at 125°C and approximately 1.973 GPa.

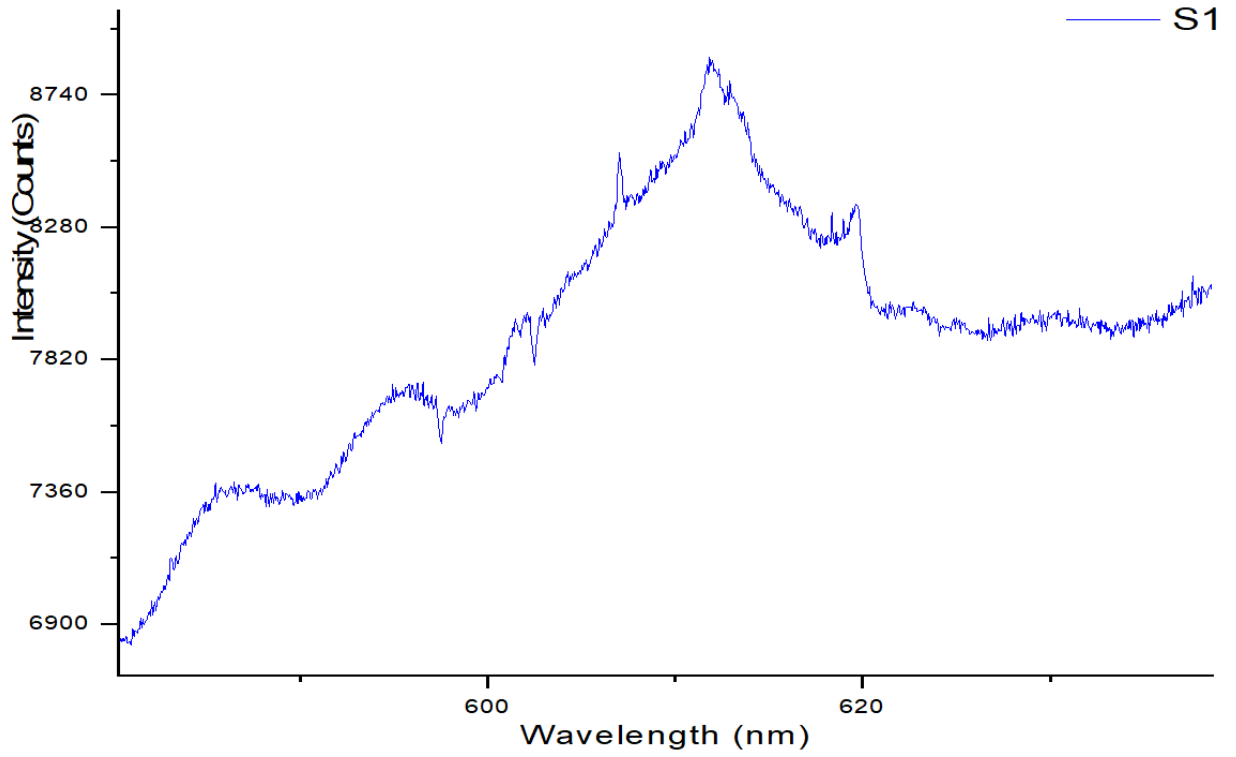

1.6: A nitrogen spectrum collected at 125°C and approximately 1.055 GPa.

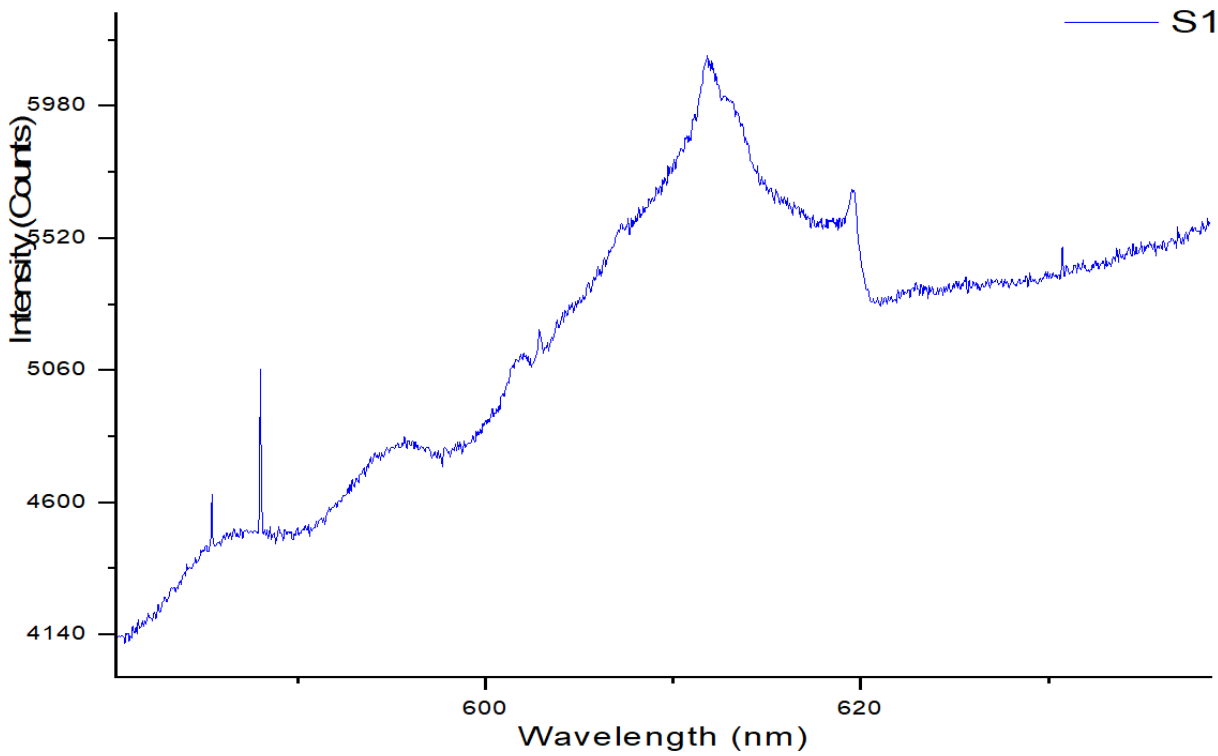

1.7: Finally, a spectrum collected at 125°C and ambient pressure. As the DAC has been opened and the supercritical nitrogen has been vented, no distinct nitrogen Raman peak is visible. A spectrum like this eventually appeared in of every experiment and indicated that no more data could be extracted from that sample. At this point, the experiment ends and the DAC is re-prepared with a cleaning, a new gasket and a new load of liquid nitrogen.

Appendix 2: The following will show two examples of ruby fluorescence spectra (*A* and *B*, respectively), one taken before and after a nitrogen spectrum reading such as those in **Appendix 1** and their resulting data. Another example can be seen in **Figure.7** of the main paper.

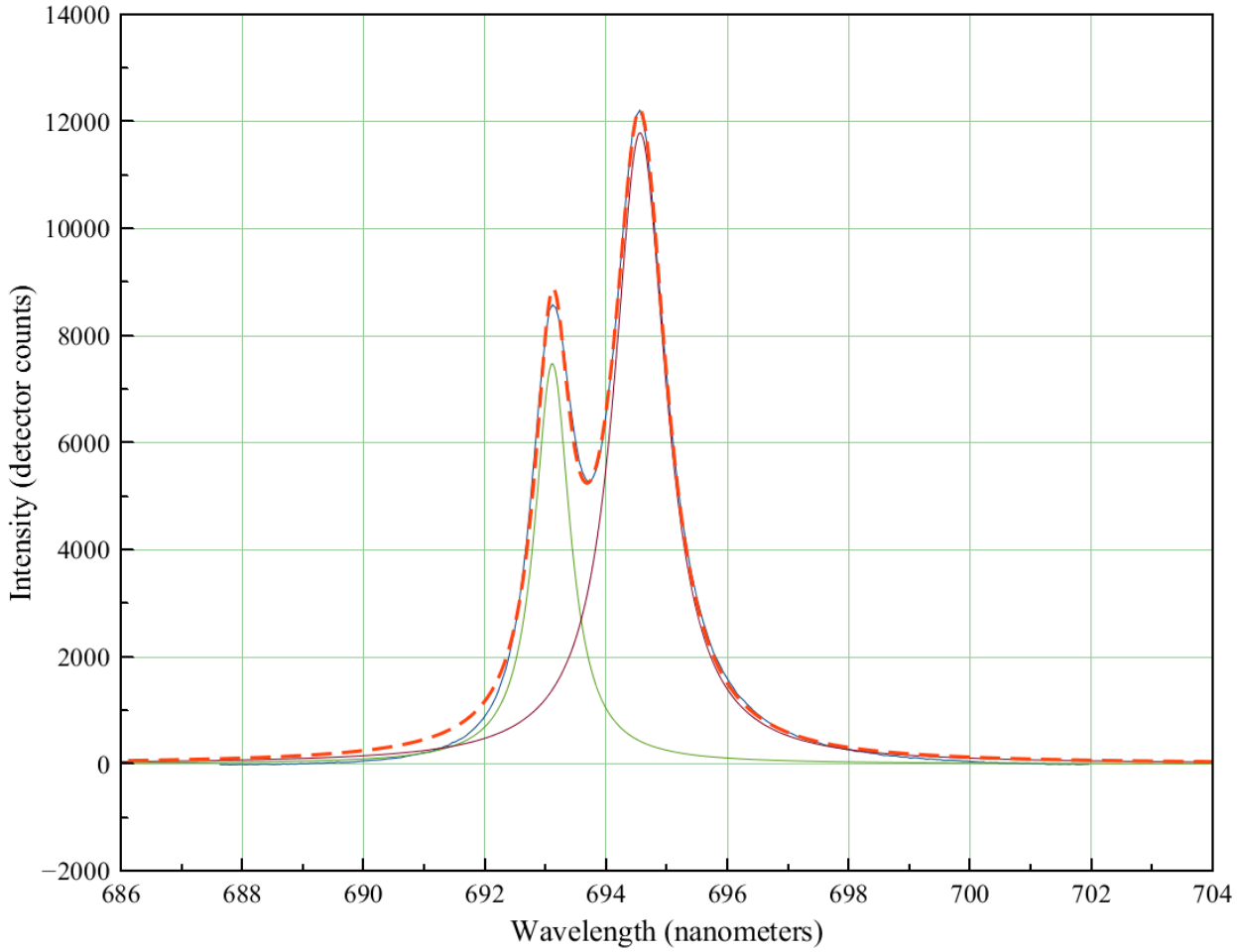

2.1: Reading *A*, taken before a nitrogen Raman spectrum reading at 77°C. Wavelength of the higher peak, on the right, was used to calculate pressure. Each has been fitted with a Lorentzian curve, the center of which was assumed to be the discrete fluorescence wavelength for that peak.

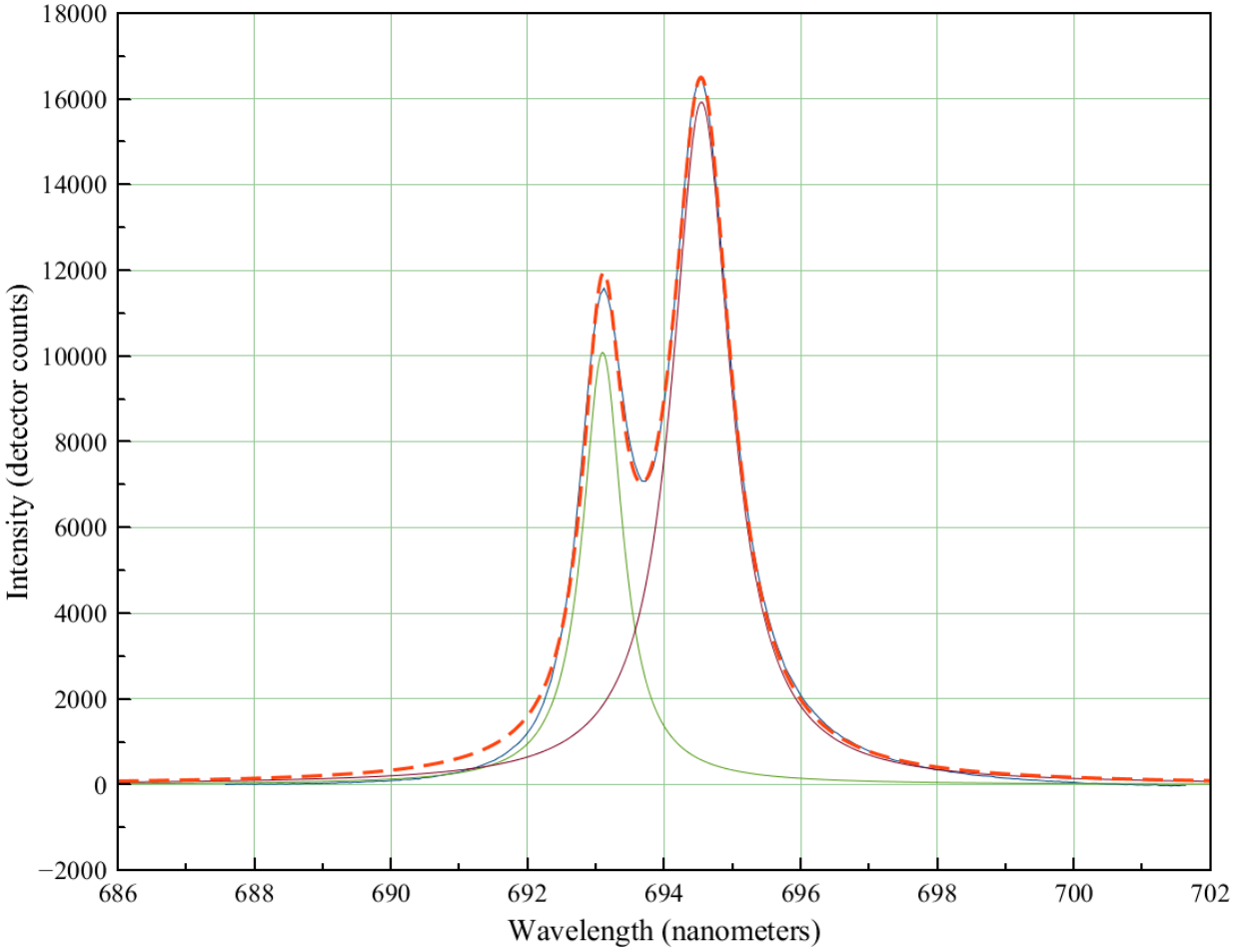

2.2: Reading *B*, taken after a nitrogen Raman spectrum reading at 77°C.

Dataset	λA *(nm)*	λ*B (nm)*	Meanλ	Temp °C	Δλ	Δλ/λ$_o$	Pressure (GPa)	ΔPressure (GPa)
R	694.5579	694.5449	694.5514	77	0.0849	0.0001222 521173	0.2287688 079	0.013

2.3: The tabulated pressure data calculated from the two spectra above, taken from a larger table of pressure calculations. This has been chosen as representative as pressure scale spectra are too numerous to include (approximately 100). The wavelength λ$_o$ is the mean wavelength for the ambient reading (the reading in which the Raman spectrum shows no nitrogen peak, as in **Appendix 1.7**). ΔPressure is the change in pressure since the last reading; in other words, since the last pressure adjustment on the lever arm. Effort was taken to minimise the change during experiments, especially around the pressure the Frenkel line encounter was expected to occur. Rough pressure calculations were performed mid-experiment to predict this.

Appendix 3: The following will be similar to **Appendix 2**, showing two examples of Sm:YAG fluorescence spectra, one before and after a nitrogen Raman spectra reading (again, *A* and

B). These spectra were yet more numerous than those of ruby with easily 200 individual spectra.

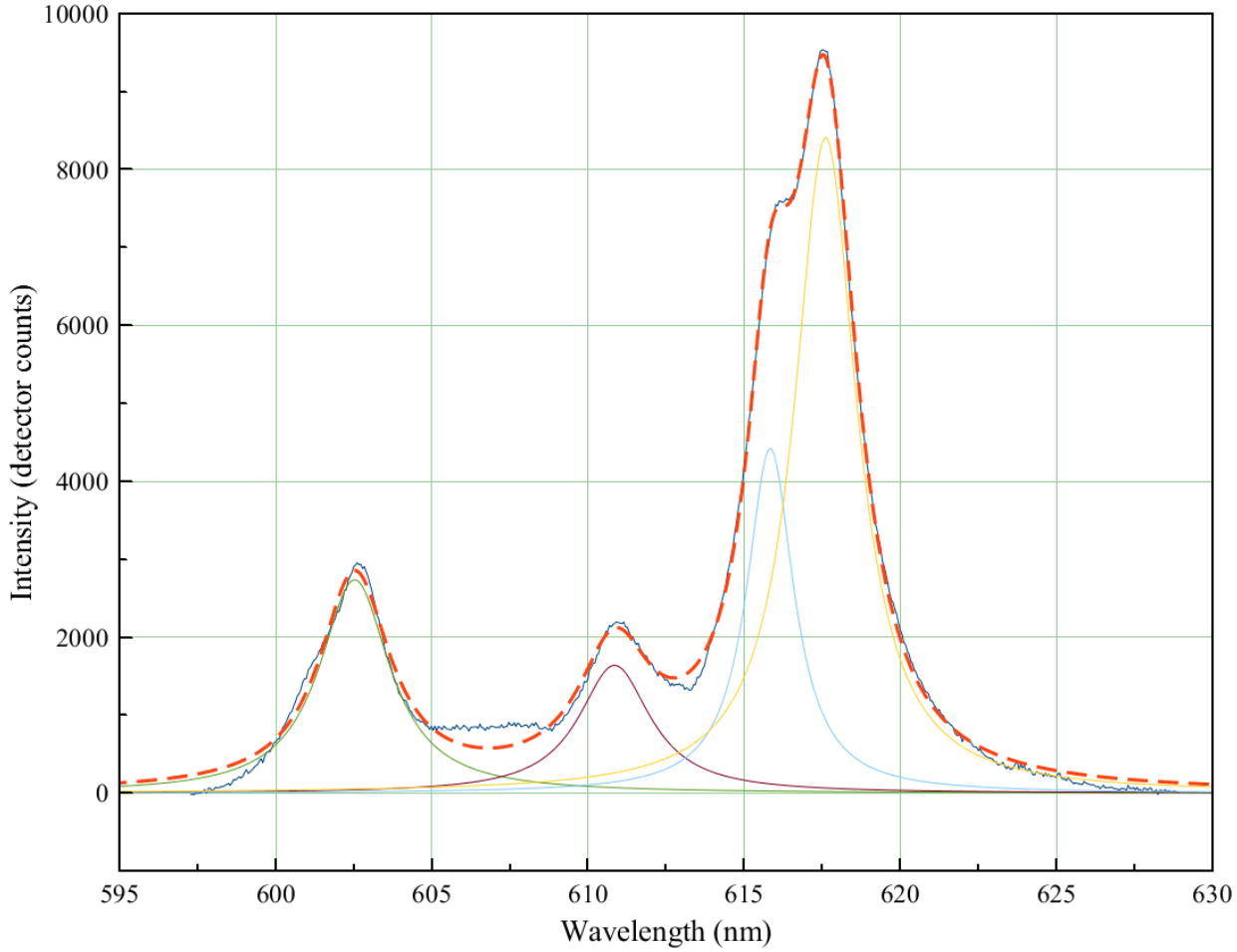

3.1: Reading *A*, taken before a nitrogen Raman spectrum reading at 100°C. The visible peaks, from left to right, are *Y4*, *Y3*, *Y2* and *Y1*. Like the ruby spectral peaks, each has been fitted with a Lorentzian curve. While the combination of these four curves does not perfectly match the spectrum, especially at its lower wavelengths, it does conform to the shape of *Y1* and *Y2* well enough to determine the wavelength at the center of these two peaks. The wavelength of *Y1* was used for pressure calculations in all experiments using Sm:YAG.

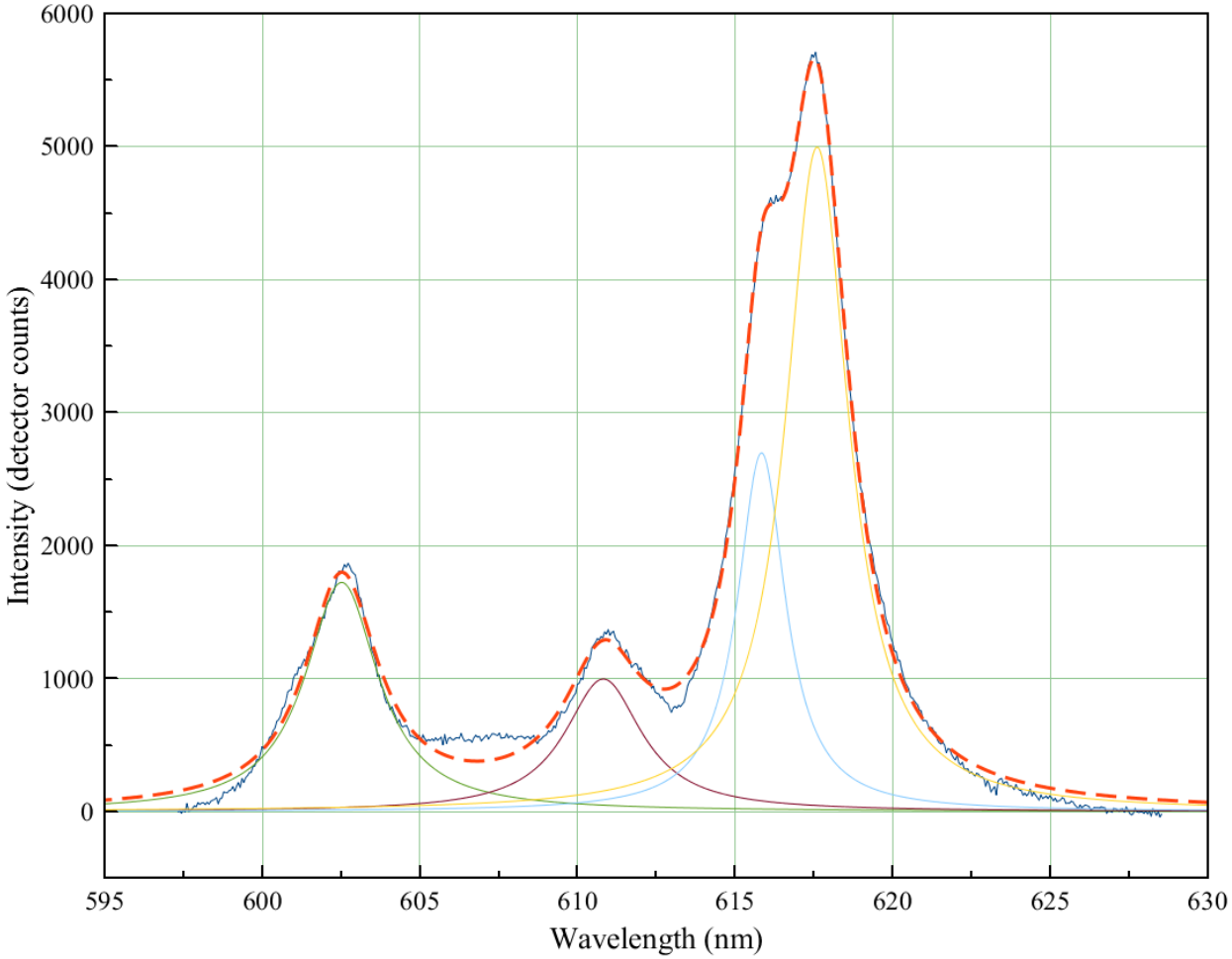

3.2: Reading *B*, taken after a nitrogen Raman spectrum reading at 100°C.

Dataset	λA *(nm)*	λ*B (nm)*	Meanλ	Temp °C	Δλ	$\Delta\lambda/\lambda_o$	Pressure (GPa)	ΔPressure (GPa)
I	617.6113746	617.6056552	617.6085149	100	0.08197978703	0.000132755084	0.2484375534	0.005719384065

3.3: The tabulated data calculated from the two Sm:YAG spectra shown previously.

References:

[1] Schlosky, K. “Supercritical phase transitions at very high pressure”. J. Chem. Educ. **1989**, 66, 12, 989

[2] Brazhkin, V.V. et al. “Two liquid states of matter: A dynamic line on a phase diagram” Phys. Rev. E, **2012**, 85, 031203

[3] Faghri, A.; Zhang, Y. “Transport Phenomena In Multiphase Systems”; Academic Press, **2006**, p5-7.

[4] Proctor, J, E;. “The Liquid and Supercritical Fluid States of Matter”, Taylor & Francis Group, **2020**, *Chapter 6.1 The Widom Lines*

[5] Brazhkin, V, V et al.; “Comment on “Behavior of Supercritical Fluids across the Frenkel Line”” . J. Phys. Chem. B **2018**, 122, 22, 6124–6128 (Further sources included in cited paper)

[6] Brazhkin, V.V.; Lyapin, A.G.; Ryzhov, V.N. et al. “The Frenkel line and supercritical technologies”. Russ. J. Phys. Chem. B, **2014**, 8, 1087–1094

[7] National Institute of Standards and Technology. (n.d.). “Thermophysical Properties of Fluid Systems”. *https://webbook.nist.gov/chemistry/fluid/*

[8] Span, R.; Lemmon, E.W.; Jacobsen, R.T.; Wagner, W.; Yokozeki, A. “A Reference Equation of State for the Thermodynamic Properties of Nitrogen for Temperatures from 63.151 to 1000 K and Pressures to 2200 MPa”. J. Phys. Chem. Ref. Data, **2000**, 29, 6, 1361-1433

[9] Pruteanu CG, Proctor J.E., Alderman O.L.G., Loveday J.S. “Structural Markers of the Frenkel Line in the Proximity of Widom Lines”. J Phys Chem B. **2021**;125 :8902-8906.

[10] Proctor, J, E et al,; “Transition from Gas-like to Liquid-like Behavior in Supercritical N2” J. Phys. Chem. Lett. **2019**, 10, 6584−6589

[11] Proctor, J, E,; Massey, D. “Electric discharge machine for preparation of diamond anvil cell sample chambers”. Review of Scientific Instruments, **2018**, 89, 105109

[12] Lorenzana, H, E et al.; “Producing diamond anvil cell gaskets for ultrahigh-pressure applications using an inexpensive electric discharge machine” Review of Scientific Instruments, **1994**, 65, 3540

[13] Proctor, J, E,; Spender, J, E,; Gould, H,T . “Phase Diagram of Ethane above 300 K” J. Phys. Chem. C, **2022**, 126, 10792−10799

[14] Shen, G et al.; “Toward an International Practical Pressure Scale: A Proposal for an IPPS Ruby Gauge (IPPS-Ruby2020)”. High Press Res. **2020**, 40, 299−314.

[15] Trots, D. M.; Kurnosov, A.; Ballaran, T. B.; Tkachev, S.; Zhuravlev, K.; Prakapenka, V.; Berkowski, M.; Frost, D. J. “The Sm:YAG Primary Fluorescence Pressure Scale” J. Geophys. Res.: Solid Earth **2013**, 118, 5805-5813.

[16] Innokenty Kantor (n.d.). “Fluorescense pressure calculation and thermocouple tools”. http://kantor.50webs.com/ruby.htm

[17] Huang, T et al,; “Ruby spectral bandprofile analysis for temperature sensing”. J. Appl. Phys. **1994**, 75, 3599

[18] Zhao, Y et al.; “Pressure measurement at high temperature using ten Sm:YAG fluorescence peaks”. J. Appl. Phys. **1998**, 84, 4049

[19] Fanjoux, G.; Millot, G.; Lavorel, B. “Collisional Shifting and Broadening Coefficients for the Rovibrational Anisotropic S(J) Lines of Nitrogen Studied by Inverse Raman Spectroscopy”. J. Raman Spectrosc. **1996**, 27: 475-483

[20] Mikhailov, G. V.; "The influence of temperature and pressure on the Raman spectrum of nitrogen". Soviet Physics JETP, **1959**, 36.9 .

[21] Nienhuis, G.; Schuller, F. “Collision and Doppler broadening of fluorescence and Raman scattering from atoms”. Physica 92C, **1977**, 409-420

[22] Abdellatif, G.; Imam, H.; “A study of the laser plasma parameters at different laser wavelengths”. Spectrochimica Acta Part B, **2002**, 57, 1155-1165

[23] Proctor, J, E;. “The Liquid and Supercritical Fluid States of Matter”, Taylor & Francis Group, **2020**, *Appendix D*

[24] Proctor, J, E;. “The Liquid and Supercritical Fluid States of Matter”, Taylor & Francis Group, **2020**, *Appendix B, B.6. Phase Diagram of N2*